

# **WATER FLUSHING OF ROCK CHIPS FROM HORIZONTAL HOLES DRILLED BY ROTARY PERCUSSION**

**Arthur Mark Kilfoil**

**A project report submitted to the Faculty of Engineering,  
University of the Witwatersrand, Johannesburg, in partial  
fulfilment of the requirements for the degree of Master  
of Science in Engineering.**

**Rooдеpoort, 1997**

## DECLARATION

I declare that this project report is my own, unaided work. It is being submitted for the degree of Master of Science in Engineering in the University of the Witwatersrand, Johannesburg. It has not been submitted before for any degree or examination in any other University.

\_\_\_\_\_  \_\_\_\_\_

\_\_21\_\_<sup>st</sup>\_\_\_\_\_ day of \_\_OCTOBER\_\_ 1997

## ABSTRACT

The flushing flow rate required to maximise penetration rate of holes drilled by rotary percussion is dependant on drilling parameters and chip size. Experimental work to determine the optimal flushing water flow rate for two common drilling situations was undertaken. It consisted of drilling, analysis of chip samples and flow visualization. A computer model to predict flow rate was developed. Its output and the experimental results were combined to explain the relationship between penetration rate and flow rate.

All chips should be flushed from the gap between the bit and the end of the hole in the time between hammer blows (ie. - within the duration of a percussion cycle). As flow rate increases, flushing improves and therefore penetration rate increases. Once flushing is adequate there is no mechanism for further increases in penetration rate, thus it remains constant and independent of further increases in flow.

## ACKNOWLEDGEMENTS

I would like to thank the following:

1. The management of my employer, Boart Longyear Research Centre for granting permission to publish this research which was carried out using Boart Longyear facilities.
2. My supervisor, Associate Professor A.E. Moss, for his valuable advice, insights and comments.
3. Those members of staff at Boart Longyear Research Centre who performed some of the experimental work, in particular Joel Molepolle, whose expert operation of the rockdrills and good understanding of the requirements of the research was invaluable.
4. Ian Schwartz, consulting metallurgist, retained by Boart Longyear Research Centre, for his very useful and practical suggestions on measurement methods and chip sampling.

# CONTENTS

	Page
DECLARATION	ii
ABSTRACT	iii
ACKNOWLEDGEMENTS	iv
CONTENTS	v
LIST OF FIGURES	vii
LIST OF TABLES	ix
LIST OF SYMBOLS	x
NOMENCLATURE	xii
1 INTRODUCTION	1
1.1 Rock Drilling	1
1.2 Relevance of Chip Removal to the Drilling Process	4
1.3 Criteria for Optimum Flow Rate	5
1.4 Objectives	6
1.5 Approach Adopted and Organisation of Report	6
2 REVIEW OF LITERATURE AND DRILLING PRACTICE	8
2.1 Flushing	
2.1.1 Public domain material	8
2.1.2 Restricted material	9
2.2 Drilling Industry Norms	11
2.3 Closely Related Topics	13
3 EXPERIMENTATION	14
3.1 Hydraulic Rockdrill using a 48 mm Diameter Bit	14
3.1.1 Site and equipment	14
3.1.2 Procedure	15
3.1.3 Calibration and observations	16
3.1.4 Data processing	19
3.2 Pneumatic Rockdrill using a 36 mm Diameter Bit	19
3.2.1 Site and equipment	19
3.2.2 Procedure	21

3.2.3 Observations	22
3.2.4 Data processing	23
3.3 Chip Size Analysis for Both Bits	23
3.4 Flow Visualisation	24
3.4.1 Apparatus	24
3.4.2 Experimental method and data analysis	25
3.4.3 Effect of rotational speed	26
3.5 Flow/Pressure Relationship	28
 4 COMPUTER MODEL	 29
4.1 The Necessity of Modelling	29
4.2 Overview	29
4.3 Modelling Procedure	30
4.4 Inputs and Outputs	32
 5 RESULTS AND DISCUSSION	 35
5.1 Chip Samples	35
5.1.1 Size, shape and size distribution	35
5.1.2 Implications of size distribution	40
5.2 Flow and Penetration Rates	44
5.2.1 Absolute minimum flow rate	47
5.2.3 Explanation for penetration and flow data	48
5.3 Flow Rate and Scatter in Penetration Rate Data	60
5.4 Initial Chip Position and Flow Rate	62
5.5 Flushing Water Pressure	66
 6 CONCLUSIONS	 68
 7 SUGGESTIONS FOR FURTHER WORK	 70
 APPENDIX A EQUIPMENT AND APPARATUS	 72
APPENDIX B COMPUTER MODEL	75
APPENDIX C SUPPORTING CALCULATIONS	96
APPENDIX D DETAILED DATA	102
 REFERENCES	 115

# LIST OF FIGURES

Figure	Page
1.1 Drilling system	1
1.2 Button bit in a hole	2
1.3 Typical button bit	3
1.4 Fluid and chip flow	4
3.1 Arrangement for drilling at West Wits	14
3.2 Water supply systems	15
3.3 Arrangement for drilling into concrete blocks	20
3.4 Bit and drill rod in glass tube	25
3.5 Flow over the bit	26
3.6 Observing flow with the bit rotating	27
3.7 Outward flow from the flute flushing holes	28
4.1 Flow chart for the computer model	34
5.1 Typical chip shapes	36
5.2 Effect of flow rate on chip size	39
5.3 Effect of penetration rate on chip size	44
5.4 Effect of flow rate on penetration rate	46
5.5 Flushing fluid passage through the pneumatic rockdrill	51
5.6 Modification to the equipment for the 36 mm diameter bit	52
5.7 Fluid coverage at 3.9 l/min.	55
5.8 Fluid coverage at 4.8 l/min.	56
5.9 Flushing of different sized chips	58
5.10 Scatter in penetration rate data	61
5.11 Chip and fluid velocities	65
5.12 Water pressure	67
B1 Kinked reference plane	78
B2 Co-ordinate system	79
B3 Approximation to hemispherical button shape	81
B4 Approximation to conical button shape	82

B5	Clearances for the 48 mm diameter bit	83
B6	Probable flow pattern for the 48 mm diameter bit	85
B7	Probable flow pattern for the 36 mm diameter bit	85
B8	Programme listing	90
B9	Sample input and output	94
D1	Drilling data for the 48 mm diameter bits	104
D2	Velocity of flushing water and very large flat chip	108
D3	Chip displacement	108
D4	Velocity of flushing water and minute cubic chip	109
D5	Effect of chip size on velocity	110



# LIST OF TABLES

Table	Page
3.1 Typical observations, 48 mm diameter bit and hydraulic rockdrill	17
3.2 Sample observations, 36 mm diameter bit and pneumatic rockdrill	23
F 1 Properties of large chips	37
D1 Drilling data for 36 mm diameter bits	102
D2 Summary of drilling data for 48 mm diameter bits	103
D3 Results from the model for the 48 mm diameter bit	106
D4 Results from the model for the 36 mm diameter bit	111
D5 Chips produced by the 36 mm diameter bits	112
D6 Chips produced by the 48 mm diameter bits	113

# LIST OF SYMBOLS

Symbol	Quantity
$a$	Acceleration
$aa$	Angular component of chip acceleration
$ar$	Radial component of chip acceleration
$A$	Cross sectional area
$A_s$	Surface area
$A_t$	Total surface area of chips
$ced$	Chip equivalent diameter
$C_d$ or $C_d$	Drag coefficient
$cx1$ to $cx5$	Effective gap (clearance) between the end of the bit and the end of the hole
$d$	Internal diameter (bore) of cylinder
$D$	Hole diameter
$E$	Percussion energy input to the hole
$f$	Rockdrill percussion frequency
$F$	Feed force on rockdrill
$k$	Constant
$i$	Counter in model
$iQ$	Flow rate increment
$it$	Time increment
$l$	Hole length
$m$	Chip mass
$n$	Number of
$N$	Bit rotational speed
$p$	Penetration rate
$P$	Pressure in feed cylinder
$r$	Distance from axis of bit to centre of flushing hole or radius of spherical chip with volume equal to that of a typical non-spherical chip
$R1$ to $R5$	Radii to annular areas on the face of the bit
$R_s$ or $Re$	Reynold's number of chip in the fluid
$Res0$	Reynold's number of the chip in the fluid at its initial position ( $s0$ )
$s$	Chip position (relative to the centre line of the bit) at the end of any time step
$s0$	Initial radial position of chip

sa	Circumferential displacement of chip
sr	Radial displacement of chip or radial co-ordinate of chip position
srmax	Distance which the chip has to move to reach the annulus
t	Elapsed time
u	Velocity of chip as it is formed on the end of the hole
$v_i$	Circumferential velocity imparted to the water by bit rotation
vc	Chip velocity
vca	Circumferential component of chip velocity
vcr	Radial component of chip velocity
vf	Fluid velocity
vfs0	Fluid velocity at radius at which chip is formed
vfa	Circumferential component of chip velocity
vfr	Radial component of chip velocity
$v_j$	Axial or jet velocity of water leaving a flushing hole
V	Volume
$V_s$	Volume of a typical chip
$V_h$	Volume of hole
q	Flow rate from the face flushing hole only
Q	Volume flow rate
Q1	Initial value of Q in the model
QB	Volume flow rate for optimal flushing
x1 to x5	Effective clearance factor
y	1 - blockage due to chips
dE/dt	Percussion power input to the hole
dl/dt	Penetration rate
$\beta_3$ or beta3	Gauge angle of bit
$\mu$ or vis	Dynamic viscosity
$\pi$ or Pi()	Ratio of the diameter of a circle to its diameter
$\rho$ or rho	Density
$\omega$	Angular velocity of the bit

## NOMENCLATURE

**BUTTON** : Cylindrical item inserted into rotary percussion drill bits to transmit drilling energy from the rest of the bit to the material being drilled. Typically made from cemented tungsten carbide because of its hard wear resistant nature.

**BUTTON BIT** : Drill bit fitted with buttons.

**CHIP or CHIPPING** : Piece of loose material produced by the action of the drill bit on the material being drilled.

**COLLAR DEPTH** : Depth of the initial part of the hole during which the rockdrill was operated at reduced power to enable the bit to start drilling slowly. If the hole is not started slowly the bit will often deviate to one side instead of penetrating.

**DRILL RIG** : Machine containing one or more rockdrills. It is used to move the rockdrills into position as well as provide thrust while holding the rockdrills steady during drilling.

**DRILL ROD** : Long hollow length of steel used to transmit drilling energy from a rockdrill to a drill bit.

**DRILLING ENERGY** : Energy in a form suitable for drilling.

**FEED FRAME** : Part of a drill rig to which a rockdrill is connected. It provides the thrust or feed force which is needed for drilling.

**FLOW VISUALIZATION** : Observation of flow over the face of the bit and the end of the hole.

**FLUSHING** : Removal of chips from the hole.

**PENETRATION RATE** : Linear velocity of the drill bit into the medium being drilled.

**PERCUSSION** : Impact energy produced in the rockdrill. Also called hammer blows.

**QUARTZITE** : Most common rock type in South African gold mines and particularly on the Witwatersrand. It is very hard, strong and abrasive.

**REGRINDING** : Process whereby chip size is reduced as the chip is flushed out of the hole.

**RESIDENCE TIME** : Period during which a chip is in the gap between the end of the bit and the end of the hole.

**ROCKDRILL** : Machine which converts fluid energy (usually contained in flows of compressed air or high pressure hydraulic oil) into a form suitable for drilling - typically percussion and/or rotation.

**ROTARY PERCUSSION DRILLING** : Use of a combination of rotation and percussion at the bit to produce penetration. It is the best (fastest and cheapest) drilling technique for hard brittle materials such as most rock types.

**SLIP VELOCITY** : Difference between the velocity of the flushing fluid and the velocity of a chip.

**WATER SWIVEL** : Device for getting a water supply into a rotating drill rod, while leaving both ends of the drill rod free for transmission of percussion.

# CHAPTER 1

## INTRODUCTION

### 1.1 ROCK DRILLING

Many current mining, and to a lesser extent construction, methods are dependent on drilling of holes in hard brittle materials such as rock and concrete. The most common technique for drilling such holes, especially in hard and/or strong rock is rotary percussion. It is so named because the drill bit is simultaneously rotated and hammered against the material being drilled (usually rock). A number of different variants of rotary percussion drilling exist, but the most common is probably that illustrated in figure 1.1.

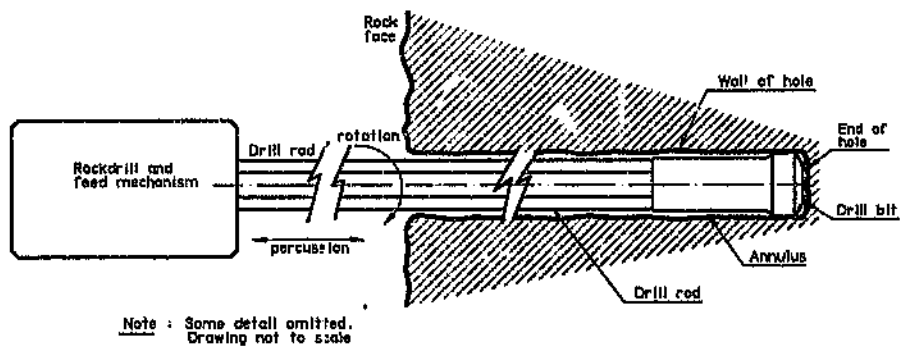


Figure 1.1 Drilling system

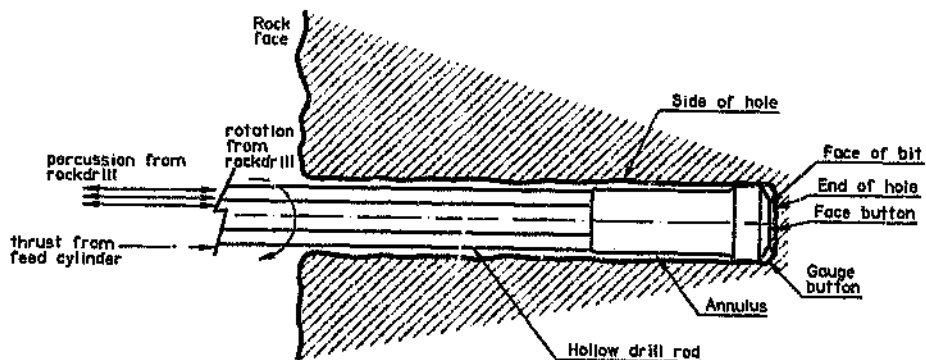
The material being drilled is broken into small pieces (called "chips" or "chippings") by the action of the drill bit (often referred to simply as the bit). The rockdrill provides the energy needed for drilling. As shown, the bit is connected to the rockdrill by one or more hollow rods or tubes, hereafter referred to as "drill rods".

The main rock breaking mechanism is the percussion, often called hammer blows or impacts. It is produced in the rockdrill by impact of its reciprocating piston on the last drill rod. The percussion is transmitted to the bit as stress waves which travel along the drill rod/s. The stress waves travel through the bit into the material at the end of the hole (see figures 1.1 and 1.2). Rotary percussion drilling is therefore a high frequency intermittent process.

Other equipment outside the hole applies an axial force (thrust or feed) through the drill rod/s to the bit. Thus, the bit is always in contact with the end of the hole.

The button bit is the most common type. As shown in figure 1.3, it consists of cylindrical cemented tungsten carbide buttons in a steel body. Only the buttons are normally in contact with the rock; therefore they transmit the percussion to the rock. Buttons are made with various profiles, eg. hemispherical, conical, parabolic, on their protruding ends.

The main function of rotation is to ensure that the buttons on the bit come into contact with different parts of the end of the hole.



Note : Some detail omitted

**Figure 1.2 Button bit in a hole**

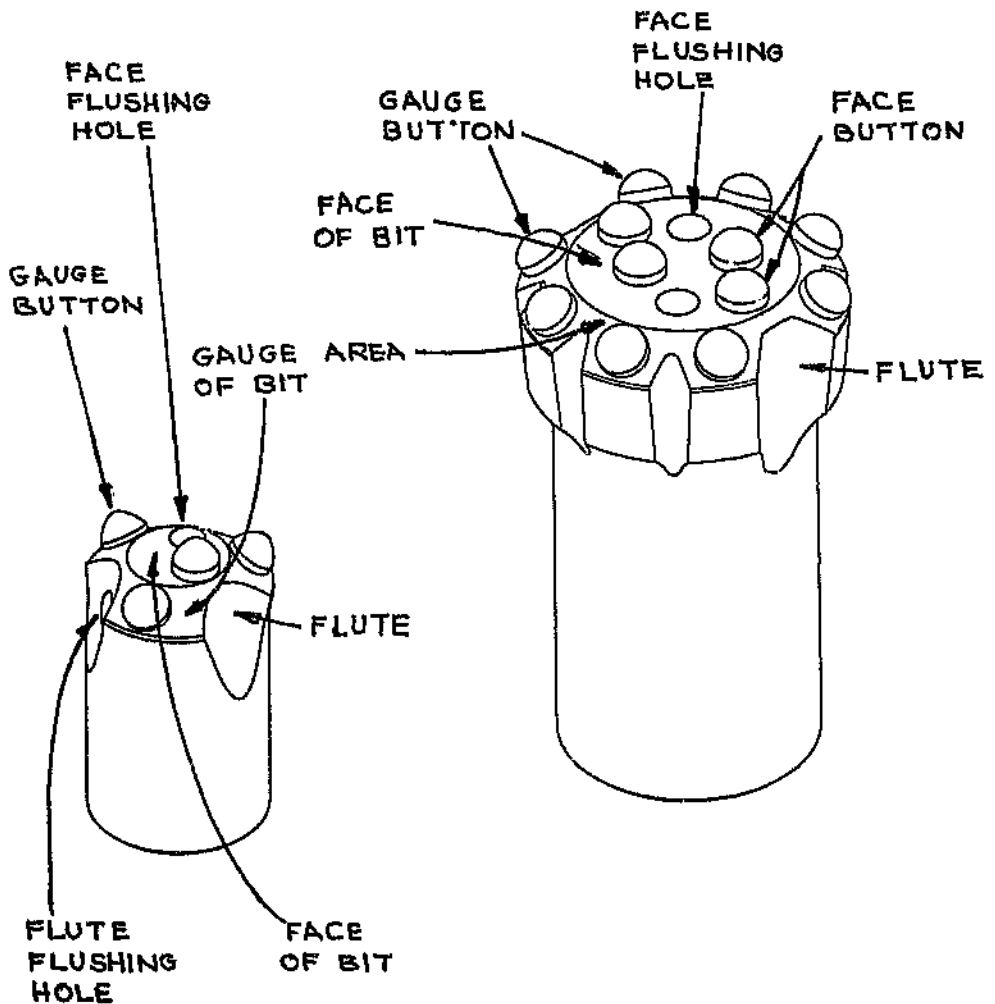


Figure 1.3 Typical button bits

All rock drilling processes break the rock into small pieces (chips). These are produced by the bit at the end of the hole as it penetrates into the rock ahead of it. The design of button bits results in chips being produced only where the buttons are in contact with the end of the hole. Since percussion is cyclic, chips are only produced when the stress waves from the percussion arrive at the end of the hole.



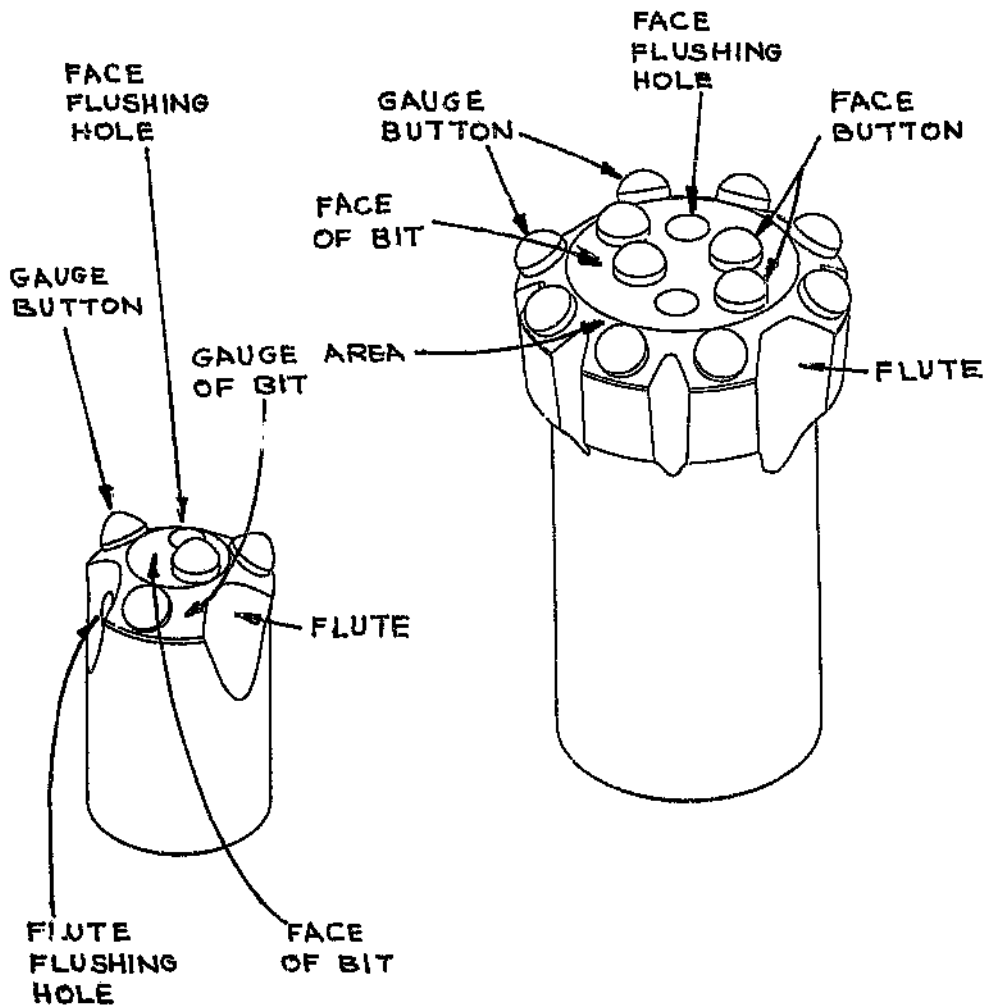


Figure 1.3 Typical button bits

All rock drilling processes break the rock into small pieces (chips). These are produced by the bit at the end of the hole as it penetrates into the rock ahead of it. The design of button bits results in chips being produced only where the buttons are in contact with the end of the hole. Since percussion is cyclic, chips are only produced when the stress waves from the percussion arrive at the end of the hole.

## 1.2 RELEVANCE OF CHIP REMOVAL TO THE DRILLING PROCESS

As with any drilling operation the material separated during the process has to be removed from the hole. If not, loose material will build up between the drilling tool and the sides and/or end of the hole. If this occurs, further deepening of the hole becomes impossible. Most rock drilling processes use a fluid to continuously remove the chips as the hole progresses.

Since a fluid is used, the process of removing chips from the hole is called "flushing". Fluid supply is typically through the rockdrill, hollow drill rod/s and bit where it saves through flushing holes.

It is readily apparent from figure 1.4 that flushing consists of two stages. First, newly formed chips between the end of the hole and the face of the bit enter the flow, which conveys them to the annulus between the drill rod/s and the sides of the hole. Second, they move along the annulus and out of the hole. The flow between the bit and the end of the hole is very different from that in the annulus between the drill rod/s and the sides of the hole.

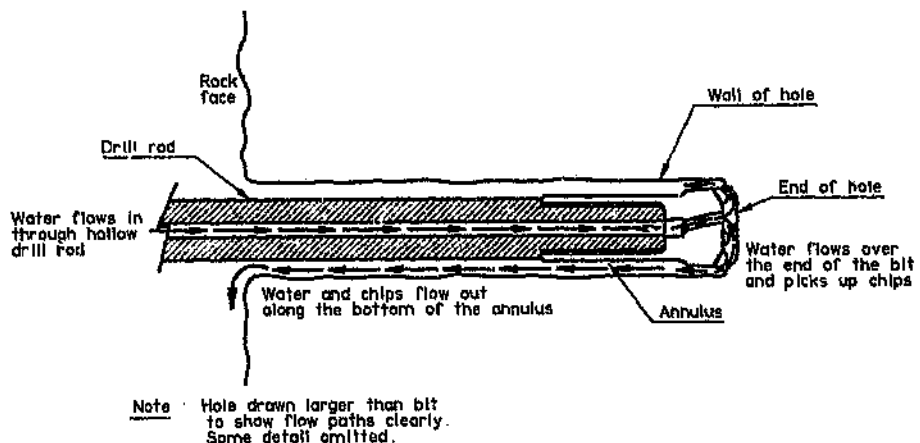


Figure 1.4 Fluid and chip flow

Both stages are equally important. However, this research only deals with the first stage ie. chip movement from the end of the hole to the annulus. The situation in the annulus is much simpler and therefore relatively well understood.

Most rotary percussion drilling, especially for small diameter holes, is done using water as a flushing medium. Thus this research concentrated on water flushing.

Many of the chips formed by button bits are large, ie. - their longest dimension is often greater than 10 % of the diameter of the hole. However for various reasons their size may be reduced before they leave the hole. This process is usually called "regrinding".

In the drilling industry it is common knowledge that if flushing flow is inadequate, drilling will be slower than it otherwise could be. In other words, the penetration rate of the bit into the rock will be low. However the causes of low penetration are poorly understood. Also, scientific determinations of optimum flow rates are seldom undertaken. Thus the industry survives on trial and error. Even when the optimum flow for a particular application is known, there is no basis for generalising this knowledge to any other situation.

### 1.3 CRITERIA FOR OPTIMUM FLOW RATE

The commercial criterion for efficient drilling of holes (in any diameter) is minimum cost per unit depth of hole. Many costs (eg. wages, depreciation of equipment) accrue on a time basis and are fixed in the short term. Hence there are financial incentives to reduce the time spent on each hole by trying to increase penetration rate. The cost of drilling consumables is different, because it depends on usage not time. In the short term, expenditure on consumables is usually more controllable than most other costs. Therefore

the most common objective is to increase penetration rate while reducing expenditure on consumables. Penetration rate is immediately visible and controllable. Thus it is the focus of most attention.

Previous work has shown that if flushing flow rate is increased from zero, penetration rate increases with it, but only up to a point (see section 2.1.2). Eventually penetration rate remains constant irrespective of further increases in flow rate (at least within the limits of practicality). Thus, optimum flushing flow rate was defined as the lowest flow at which penetration rate is a maximum. It is the flow which minimizes the drilling time per hole.

#### 1.4 OBJECTIVES

The research was limited to horizontal holes drilled by rotary percussion using button bits and water flushing. Given the scope of the work, the objectives were as follows:

- 1.4.1 To develop an understanding of the process of flushing chips out from the end of the hole.
- 1.4.2 To determine the optimal flushing flow rate for certain specific situations.
- 1.4.3 To develop a computer model for reliably and accurately predicting the optimum flushing flow.
- 1.4.4 To obtain experimental data against which the predictions of the model may be checked.

#### 1.5 APPROACH ADOPTED AND ORGANISATION OF REPORT

From a review of literature, industry practice and research related to flushing, it appeared that:

- The requirement for effective flushing is sufficient but not excessive flow. The required supply pressure is fixed by the losses through the drilling equipment. The losses are dependent on the flow and the design of the equipment. Thus the research concentrated on flow rate.
- Flushing is similar to the hydraulic transport of solid particles in pipes. Therefore, chip movement could be modelled using the equations for the forces on a submerged particle in non-compressible flow. The computer model was developed from this.

Almost no data on flushing was available. Therefore experimental work was required to obtain information regarding the variation of penetration rate with flushing flow. Regrinding of chips is central to an understanding of the relationship between penetration and flushing flow. Thus chip samples were taken while drilling and size analysis was carried out on them.

In the drilling industry the basic unit of time is minutes not seconds. Cubic meters are not convenient for the volumes encountered during drilling, so the fluid volume is usually measured in litres. Thus centimetres per minute (cm/min) is typically used for penetration rate and litres per minute (l/min) is normally used for flow rate. These drilling industry conventions were adhered to in the report.

Given the approach outlined above, from here the report goes on to a review of literature and drilling practice. Next is a description of the experimental work and the computer model. Thereafter the results from the various sources are presented, synthesised and discussed. This section leads to conclusions and issues which could be researched in future.

## CHAPTER 2

# REVIEW OF LITERATURE AND DRILLING PRACTICE

Almost all available published work on chip flushing deals with one or both of the following:

- Chip movement in the annulus between the drill rod/s and the side of the hole.
- Broad rules of bit design to optimise flushing.

None of the literature deals with chip movement in the space between the end of the hole and the bit in much detail. The published data is not sufficient to predict the minimum flow rates required there for effective flushing.

However, a considerable body of practical experience exists in the drilling industry. It is the result of years of trial and error attempts at optimising drilling performance. Although it is seldom if ever documented and even less frequently published it is nevertheless very relevant.

### 2.1 FLUSHING

#### 2.1.1 PUBLIC DOMAIN MATERIAL

An equation for the air velocity needed to pick up chips where they are formed under the bit was developed by Davis<sup>(1)</sup>. However, picking up a chip is only the first step in transporting it to the annulus. Also the basis for the equation is unclear. Therefore its usefulness is severely limited.

Jain<sup>(2)</sup> gives a chip velocity of approximately 25 m/s after 75 mm movement but does not explain how the velocity was calculated or under what conditions it applies. Thus it cannot be used to calculate reliable flow rates. The large chip displacement is also a constraint because few holes drilled with rotary percussion equipment are large enough for chips to travel 75 mm before entering the annulus.

The lack of published information specifically on flushing indicates that:

- Either very little rigorous work has been done into chip movement in the space between the bit and the end of the hole and/or,
- Most of the research was for commercial purposes and therefore kept strictly confidential. However this seems unlikely because publicising the broad results of such work would have considerable value as a marketing tool. Since nothing of the kind has happened within the last ten years at least, it is reasonable to conclude that if such commercial research was done the results were of little value.

#### 2.1.2 RESTRICTED MATERIAL

Approximately fifteen years ago Boart Longyear Research Centre investigated chip flushing in some depth. Being commercial research the detailed results were never published. However, since the current work was sponsored by Boart Longyear, all the previous reports were available for scrutiny.

Berson<sup>(3)</sup> showed that for water flushing in horizontal holes, as flow rate was increased from zero, penetration rate increased in direct proportion until it reached a maximum. Flow rate was not increased much thereafter. For the small increase in flow that was investigated, penetration rate

remained constant. This showed the importance of flushing and what general trend to expect. However no detailed explanation of the observations was given and button bit design has advanced considerably since then. Current bit designs are very different from those used by Berson. Thus the relations he obtained is of limited use today.

During earlier research Berson<sup>(4)</sup> used laboratory apparatus to investigate how flushing is affected by drill rods and bits. His most important findings were:

- Chip size is not significantly affected by changing the size of the annular gap between the hole wall and the drill rods. Thus he concluded that any regrinding would occur at the end of the bit, not in the annulus.
- Chip size is affected by the position and size of the flushing holes in the bit. Therefore the flow over the face of the bit affects regrinding.

McFadzean<sup>(5)</sup> performed a range of experiments and calculations on chip movement. He collected chip samples from a number of holes drilled vertically downwards into quartzite. These holes were drilled using water flushing and a powerful pneumatic rockdrill. Standard (for 1980) button bits with diameters of 41 and 45 mm were used. Analysis of the samples produced the following typical characteristics for the largest chips:

volume	- 50 to 70 mm <sup>3</sup>
mass	- 0.13 to 0.18 g
dimensions	- 3.7 x 5.4 x 7.6 mm.

Intuitively the dimensions and volume too large relative to the diameter of the bits and the space available for chip movement. However most chips were very much smaller.



Measurement of settling velocity of the largest chips in water showed that their drag coefficients were between 1.3 and 1.7. Thus, McFadzean concluded that their drag was about three times that of an equivalent sphere with the same volume as the chip. Using the diameter of this equivalent sphere as the length term in the equation for Reynold's Number he showed that the settling process was at the low end of the Newton Flow regime - ie. at Reynold's Numbers between 1200 and 1400.

Berson<sup>(6)</sup> used a transparent tube partially filled with artificial chips to compare the flushing properties of different bit designs. He concluded that all flushing holes should be on the face of the bit. Although he was able to rotate the bit inside the transparent tube he did not vary the rotational speed or the flushing flow rate.

Williams<sup>(7)</sup> observed the flow past various bits. He also concluded that bits with all flushing holes on the face have better flushing characteristics than those with some holes in the flutes.

## 2.2 DRILLING INDUSTRY NORMS

For horizontal holes drilled with water flushing, some examples of the flow rates used in practice are given below. In all cases the figures are approximate. Unless otherwise specified, the information was obtained by Schwartz<sup>(8)</sup> for hydraulic rockdrills and 48 mm diameter bits.

Norwegian practise for holes drilled with 48 mm diameter bits then reamed out with 102 mm diameter bits: 150 to 160 l/min. [Brewitt<sup>(9)</sup>]

Kiruna mine in Sweden: 50 to 60 l/min.

Nygårdstangen tunnel in Norway: 50 l/min.

Hagerbach Test Gallery in Switzerland: flushing water pressure of 1.5 MPa, which is equivalent to a flow of approximately 60 l/min.

South African mines using hand-held pneumatic rockdrills with small bits (typically 32 to 42 mm diameter): flushing water pressures of 150 to 700 kPa which gives flows of about 1.4 to 3.2 l/min. [Loots<sup>(10)</sup>]

These pressures and flows may appear inconsistent. The differences are mostly caused by the routing of the flushing water from the supply hose to the drill rod.

Adaptors are fitted into the front end of hydraulic rockdrills to connect the last drill rod to the rockdrill. These adaptors have transverse slots which fit between two seals in the rockdrill. Flushing water flows through the slot into the bore of the adaptor and from there into the hollow drill rods.

No adaptors are used with hand-held pneumatic rockdrills. The flushing water flows through a long thin tube in the centre of the rockdrill and then into the hollow drill rod (see figure 5.5). Thus resistance to flow is much greater than it is for hydraulic rockdrills.

In addition to quantitative data, there are some generally accepted theories in the industry. Although these may not have an identifiable scientific base they should still be noted. The most relevant of these is that insufficient flushing retards penetration because some of the drilling energy is wasted in reducing the size of chips. Over many years, size analysis of chip samples taken for other purposes regularly confirmed this theory.

### 2.3 CLOSELY RELATED TOPICS

Although it is intimately connected with drilling, flushing is really a hydraulic or pneumatic transport issue.

There is a large body of published work on transport of solids in pipelines, some of which can be applied to chip flushing. However, the length of most solids transport pipelines means that the non-equilibrium conditions during particle pick up are insignificant and therefore they have not been much researched. Thus very little work on solids transport in pipelines was directly useful.

Partial exceptions are Wiles<sup>(11)</sup> who suggests an air speed for picking up sand in a pneumatic conveying system and shows how to calculate the pipe length required for the particles in an air stream to reach constant velocity.

Marcus et al<sup>(12)</sup> also deals with particle acceleration in pneumatic conveying. However, compressed air is typically about two orders of magnitude less dense than water. Therefore attempting to extrapolate from air to water is very dangerous.

The pipes used for particle conveying usually have constant diameter; hence fluid velocities are constant. In rock drilling the flushing fluid has to accelerate chips while its velocity is decreasing due to increasing cross sectional area as the chips get closer to the annulus.

The one other useful insight was the orientation which a solid particle will take up in a fluid. This was investigated by Bain and Bonnington<sup>(13)</sup>, Zandi and Govatos<sup>(14)</sup> and Graf<sup>(15)</sup>. They all concluded that broadside on was the most common orientation, especially in the Newton Flow range.

## CHAPTER 3

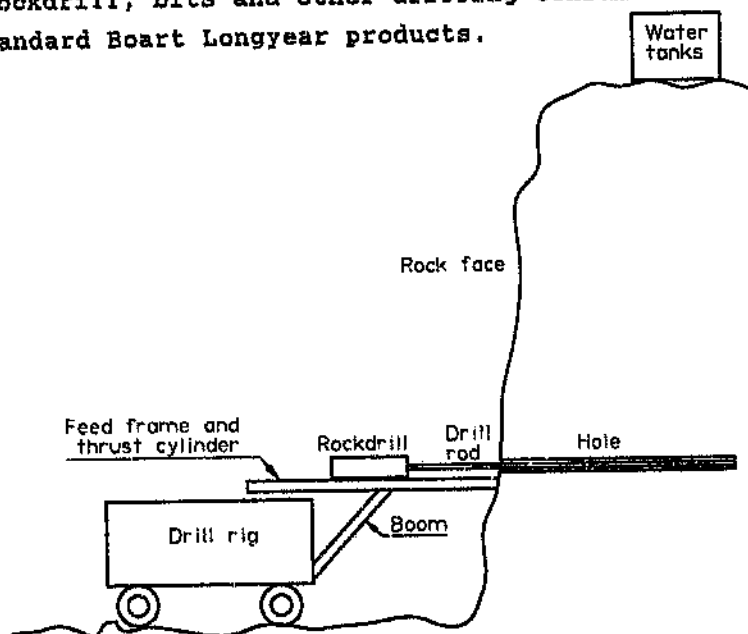
### EXPERIMENTATION

#### 3.1 HYDRAULIC ROCKDRILL USING A 48 mm DIAMETER BIT

##### 3.1.1 SITE AND EQUIPMENT

All drilling with 48 mm diameter bits was done in the North Pit at West Witwatersrand Gold Mine (hereafter referred to as West Wits). It is located between Krugersdorp and Randfontein in Gauteng, South Africa. Although it is open cast, the North Pit was excavated to access one of the Witwatersrand gold reefs. Therefore all holes were drilled into quartzite.

Figures 3.1 and 3.2 show the equipment schematically, full details of which are given in Appendix A. The drill rig, rockdrill, bits and other drilling consumables were all standard Boart Longyear products.



Note . Some detail, such as water pump and hoses omitted.  
Drawing not to scale.

Figure 3.1 Arrangement for drilling at West Wits.

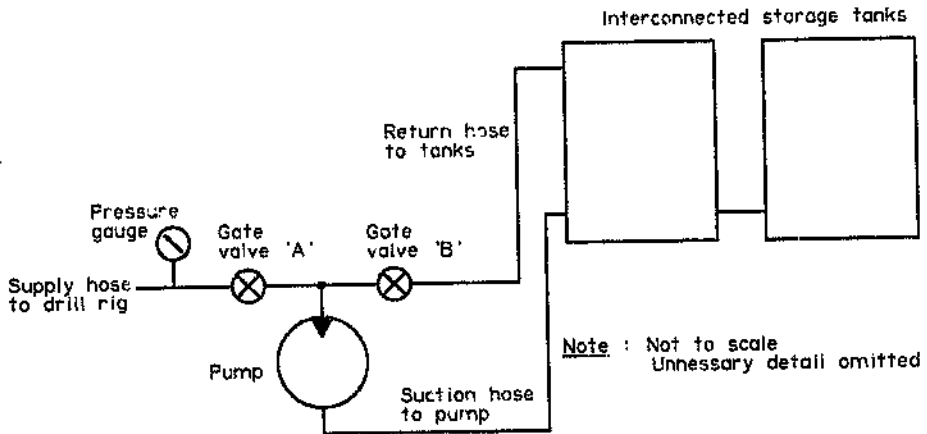


Figure 3.2 Water supply systems

The static head from the water tanks was sufficient to provide a flow rate of 14 l/min (litres per minute). For greater flows a pump was used. The tanks were approximately 20 m above the drill rig and they had a combined capacity of 10 000 l. Thus, even a full day of drilling would not result in a significant change in static head.

The water was supplied by West Wits from underground sources. Like most mine water, it was not safe to drink, but was substantially free of solids.

### 3.1.2 PROCEDURE

The important components of the experiment were as follows:

- (a) Warm up the hydraulic oil by drilling three holes with an old bit. (The performance of the rockdrill was sensitive to oil viscosity. Only when warm was the recommended grade of oil in the correct viscosity range).

- (b) The water flow rate through the bit was set by adjusting gate valve A (see figure 3.2). It was left undisturbed until the flow rate needed to be changed.
- (c) A new bit (identical to all the others) was fitted when the flow rate was changed. This ensured that at each flow rate, the bit was subject to similar wear as the bits used at the other flow rates.
- (d) In most cases ten horizontal holes were drilled at each flow rate. To minimise the effect of variation in rock properties, most holes were drilled in random positions. Ten holes were statistically acceptable while limiting the effect of bit wear.
- (e) Each hole was collared (ie. started slowly) using reduced percussion. After collaring, the percussion valve was opened fully so that the rest of the hole could be drilled at full power.
- (f) For the purpose of establishing penetration rates, the duration of full power drilling was measured. After completion, hole depth was measured and adjusted for the untimed initial portion (collar depth). The holes were typically about 2.4 m deep and drilling time varied from over five minutes to less than two minutes.
- (g) Independent variables such as percussion, rotation and feed pressures were kept constant at the values recommended by the manufacturers of the drill rig.
- (h) A sample of chips was taken from some of the holes.
- (i) After drying, the chip samples were sieved into size fractions and each fraction was weighed.

### 3.1.3 CALIBRATION AND OBSERVATIONS

Table 3.1 is an example of a typical set of observations. The constant parameters for this set of holes were:

Flushing flow rate: 20 l/min.

Feed pressure = 9 MPa; therefore thrust force on the bit was 14 kN (see appendix C)

Percussion pressure = 15.5 MPa; therefore percussion frequency was 49 Hz.

Rotation pressure = 4.5 MPa; therefore rotational speed was 197 rpm.

Table 3.1 Typical set of observations; 48 mm diameter bit and hydraulic rockdrill at 20 l/min.

Hole number	Hole depth (cm)	Drilling time (min:sec)	Penetration rate (cm/min)
1	220	1:57.32	112.51
2	240	2:07.41	113.02
3	250	2:22.64	105.16
4	250	2:09.04	116.24
5	250	2:09.04	116.24
6	255	1:48.26	141.33
7	240	2:04.73	115.45
8	235	2:04.29	113.44
9	240	2:41.32	89.26
10	245	2:07.21	115.56

Flow rate was measured using a stop watch and a plastic drum of known volume placed directly under the bit. Leakage of flushing water from the rockdrill and drill rod connections is normal. Thus, this method is more reliable and accurate than using a flow meter located upstream of the rockdrill.

Opening and closing of the valves in hydraulic rockdrills creates cyclic pressure variations in the oil supply hoses. The frequency of these pressure changes equals the percussion frequency of the rockdrill. Thus, to measure blow frequency, a pressure transducer was connected into the supply line to the percussion mechanism of the drill.

A storage oscilloscope was used to record several sets of pressure pulses. The period of each pulse was determined by multiplying the number of dots making up its trace on the oscilloscope screen with the time base setting.

According to the manufacturer of the rockdrill, the resulting average frequency was within the expected range. However, just to be sure, the calibration of the oscilloscope was checked. Since the measured percussion frequency was 49 Hz, the local mains electricity supply was the most convenient standard. Several sets of comparisons gave an the average discrepancy of 0.5 %.

Hydraulic oil pressures and flushing water pressure were measured with standard commercially available pressure gauges.

Drilling time was measured with a stop watch.

Due to their depth and position high up on the rock face, direct measurement of hole depth was not safe. However since all the relevant dimensions were known and fixed, depth could be obtained by subtraction. After completion of each hole, the distance from start of the hole to the end of the drill rig's feed frame was measured with a steel tape. Hole depth was calculated from this.

Rotational speed was measured by attaching a long length of string to the drill rod and allowing it to wind up in a known time. When the rod was stationary after drilling of the hole, the string was slowly unwound and the number of turns counted. The result was within the expected range. The advantages of this method over using a tachometer were as follows:

- It was safer, especially since almost all the lower part of the rock face already had holes drilled into it. Thus most holes were at least 1.5 m up the face.



- Its simplicity ensured that the chances of errors were very small. Even a newly calibrated tachometer can be wrong, especially when it is being sprayed with dirty water.

#### 3.1.4 DATA PROCESSING

Hole depth minus depth required for collaring was divided by drilling time to give average penetration rate for each hole (see table 3.1). As is standard in the industry this will hereafter referred to as penetration rate, with units of cm/min (centimetres per minute). Scatter in the results was assessed by comparing the standard deviations of penetration rates for each flushing flow rate with each other.

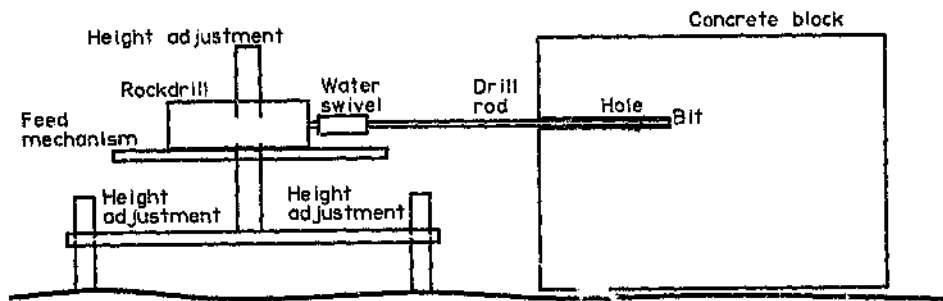
Average penetration rate for a particular bit at a particular flushing flow rate was obtained by summing the individual penetration rates and dividing by the number of holes. Since hole depth did not vary significantly, no attempt was made to apply a weighting factor.

### 3.2 PNEUMATIC ROCKDRILL USING A 36 mm DIAMETER BIT

#### 3.2.1 SITE AND EQUIPMENT

As shown in figure 3.3 the rockdrill was mounted on a special drilling platform. This ensured that all holes were drilled at the same angle (approximately  $3.2^{\circ}$  below horizontal). A standard Boart Longyear rockdrill and bits were used. Except for a small modification for a water swivel standard drill rods were used.

All flushing water was taken from the municipal supply. At the lower end of the flushing flow rate range, the water was taken directly from a tap. However, at 5 l/min and greater a pump was used.



Note : Unnecessary detail omitted  
Layout of water supply system was  
similar to that shown previously

**Figure 3.3** Arrangement for drilling into concrete blocks

As explained in section 2.2, small hand held rockdrills are not designed for high flushing flow rates. The flushing fluid is supposed to pass through a long thin tube running down the centre the rockdrill. Thus large flows require high pressures; for example at a supply pressure of 2 MPa, the flow was 7.8 l/min. Also, due to the construction of these rockdrills, the supply pressure for the flushing fluid must be significantly lower than the supply pressure of the air powering the rockdrill. If not, its performance deteriorates.

The supply air pressure was 430 kPa, therefore at flow rates greater than 5 l/min the flushing water was routed directly into the drill rod (see figure 5.6). To do so the drill rod was modified to accept a water swivel. The supply hose was connected to the swivel and the water flowed through two specially drilled transverse holes into the longitudinal hole in the centre of the drill rod.

When using the water swivel a pump was used to provide a steady flow and to overcome the pressure drop in the drill rod. At flows below 5 l/min the municipal water supply pressure was adequate.

All drilling was into a block of concrete. The mix consisted of 3 parts crushed quartzite (from West Wits) to 2.5 parts sand to 1 part cement, therefore the block was a reasonable approximation of rock.

Concrete's great advantage over rock was that the mixing processes inherent in both the production of crushed quartzite and casting the block resulted in a very homogeneous material. Thus almost all the fluctuation in penetration rate was due to variation in flushing flow rate. Very little was due to inhomogeneity in the block.

### 3.2.2 PROCEDURE

This was similar to that described previously for the 48 mm diameter bits. The important parts were:

- (a) The flushing flow through the bit was set by adjusting the tap or pump speed and a gate valve.
- (b) One or two holes at each flow rate were sufficient because:
  - (i) The concrete block was very homogeneous (Nevertheless the drilling sequence was randomised), and
  - (ii) The flat surface of the block allowed hole depth to be measured to within 0.5 %.
 Since relatively few holes were drilled, the effect of bit wear on penetration rate was negligible.
- (c) Each hole was started slowly (collared) by throttling the air supply to the rockdrill. Thus the holes were straight and in the chosen positions.
- (d) After collaring, the bit and rod were retracted and the depth of the initial part of the hole (collar depth) was measured.
- (e) Drilling then resumed, and drilling time for the remaining length of the drill rod was measured.
- (f) After completion of the hole its depth was measured. Holes were typically about 1 m deep and drilling time varied from 1.5 minutes to over 3 minutes.

- (g) Except for flushing water flow rate, all independent variables were kept constant. In particular a fixed supply air pressure was used.
- (h) A sample chips was taken from some of the holes.
- (i) After drying, the chip samples were sieved into size fractions and each fraction was weighed.
- (j) After cleaning the remaining chips out of the holes, their angle to the horizontal was measured.

### 3.2.3 OBSERVATIONS

Flow rate from the bit was measured using a stop watch and a plastic drum of known volume. Leakage of about a third of the total flow from the front of the drill is an inherent characteristic of the type of rockdrill used. So, at low flow rates, when the water flowed through the rockdrill, this was the only practical method of accurately measuring flow.

Compressed air and flushing water pressure were measured with standard commercially available pressure gauges.

The manufacturers of the particular model of rockdrill have very good knowledge of how its performance varies with supply air pressure. Hence, percussion frequency and rotational speed at the measured air pressure were obtained from the manufacturers.

Drilling time was measured with a stop watch.

Collar depth and hole depth were measured with a steel tape.

Hole angle was measured using a protractor with a built-in spirit level. A drill rod was inserted into the hole to provide a surface for a protractor to rest on.

Table 3.2 is an example of a few typical observations. The parameters which were held constant were:

Air pressure at the feed cylinder = 250 kPa; therefore thrust force on the bit was 552 N (see appendix C)  
 Air pressure at the rockdrill = 430 kPa; therefore percussion frequency was 28.5 Hz and rotational speed was 124 rpm.

Table 3.2 Sample observations, 36 mm diameter bit and pneumatic rockdrill.

Water flow rate (l/min)	1.27	5.63	16.3
Collar depth (cm)	5.5	2.5	7
Full hole depth (cm)	110	?	83
Drilling time (min:sec)	1:48.29	1:30.57	1:05.16

#### 3.2.4 DATA PROCESSING

Collar depth was subtracted from full hole depth to give the depth during which the rockdrill was run at full power. The hole depth resulting from this subtraction was divided by drilling time to give average penetration rate for each hole, hereafter referred to as penetration rate.

#### 3.3 CHIP SIZE ANALYSIS FOR BOTH BITS

A set of standard wire mesh sieves was used separate each chip sample into seven size fractions. The mesh sizes were : 2.0 mm, 1.4 mm, 1.18 mm, 0.6 mm, 0.355 mm, 0.25 mm and 0.075 mm. Each fraction was weighed on a chemical balance and size fraction data was expressed in percentage terms.

In some cases a few of the chips (called very large flat) from the largest size fraction were measured with vernier callipers. The sizes were averaged and used as inputs to the computer model. Volume and cross sectional area was calculated from the dimensions. Thereafter mass was determined by using the density of quartzite.

The number of chips in the largest size fraction of a few samples were counted by hand. The average mass of a chip (called average large flat) in the largest size fraction was obtained by dividing the mass of the size fraction by the number of chips. Volume and cross sectional area were obtained using the reverse of the procedure applied to the very large flat chips.

The shape of the smallest chips (called minute cubic) was determined from observation under an optical microscope. Typical dimensions were estimated from the size of the mesh in the finest screen.

### 3.4 FLOW VISUALISATION

It was anticipated that at low flow rates the face of the bits would not be completely covered with flushing water. In other words, a free surface of water between the face of the bit and the end of the hole was expected. Initial observations failed to disprove this, therefore a small experimental facility was developed to investigate the phenomenon.

The objective was to observe how the free surface was affected by flow rate and the orientation of the bit (flushing holes in drill bits are seldom symmetrically arranged).

#### 3.4.1 APPARATUS

As shown in figure 3.4, a glass tube was used to simulate the end and sides of the hole while allowing observation of the fluid. The diameter of holes drilled with button bits is always a couple of millimetres larger than the diameter of the bit, and the glass tubes were similarly dimensioned. To improve the simulation the tubes were made long enough to fit over the bits and part of a drill rod. To provide a contrast, the bits were painted white and a small amount of domestic toilet cistern dye "Jeyes Bloo" was used to colour the water.

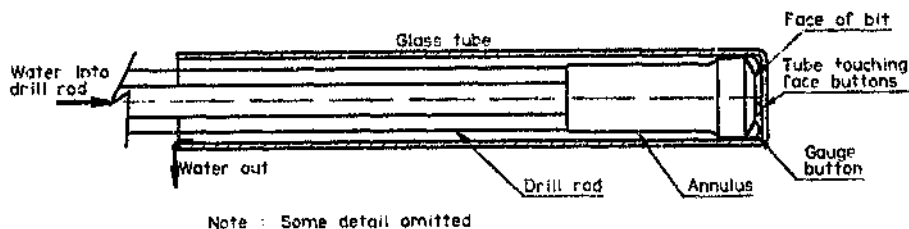


Figure 3.4 Bit and drill rod in glass tube

The remainder of the apparatus consisted of a tank for the fluid, a pump, gate valve and the necessary piping.

#### 3.4.2 EXPERIMENTAL METHOD AND DATA ANALYSIS

Flow rate was set using the valve. It was measured using a stop watch and a measuring flask.

Once the desired flow was achieved the position of the free fluid surfaces was sketched and photographed. After each observation the bit was turned (by hand) into a new orientation. The procedure was repeated at several orientations making up a full  $360^\circ$  of bit rotation.

The most interesting and varied free surface was that between the face of the bit and the end of the glass tube. There was also a free surface in the annulus between the drill rod and the glass tube. However, the annular gap is constant and independent of bit orientation. Therefore the observations concentrated on the free surface between the face of the bit and the end of the tube.

Face coverage (in percentage terms) was estimated from the position of the free surface on the face of the bit. For example, figure 3.5 depicts face coverages of 90 % (upper photograph) and 60 % (lower photograph).



Figure 3.5 Flow over the bit

#### 3.4.3 EFFECT OF ROTATIONAL SPEED

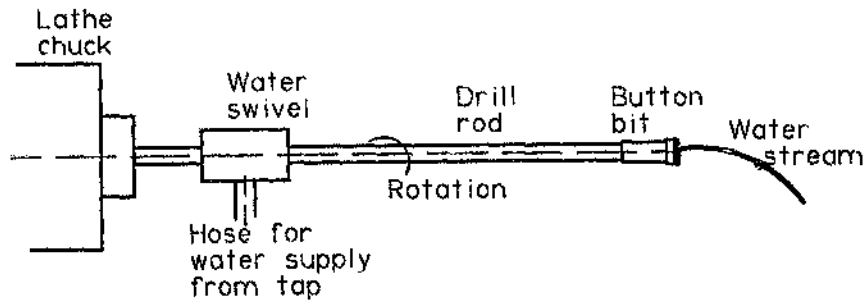
While drilling the bits were turning, but their speeds were not very high. Thus it seemed likely that rotation would have a negligible effect on how the water flowed over the bits. To be sure the hypothesis was checked by observing how water flowed out of the bits while they were rotating.

The objective was simply to assess whether bit rotation was fast enough to impart a significant outward (radial or circumferential) velocity component to the water as it left the bit. If so, observing the free surfaces with the bit stationary would have been pointless. To observe potential outward motion of the water the bits had to be rotated uncovered - ie. without a glass tube over them.

Figure 3.6 shows the experimental apparatus. After setting the water flow rate with the tap, the stream was observed while the bit was:

- stationary and,
- rotating at approximately the same speed at which the drilling experiments were conducted.





Note : Unnecessary detail omitted

**Figure 3.6** Observing flow with the bit rotating

The pneumatic rockdrill rotated at 124 rpm. The nearest available lathe spindle speed was 132 rpm, therefore it was used for the 36 mm diameter bits. Similarly, a speed of 190 rpm instead of 197 rpm was used for the 48 mm diameter bits.

These experiments suggested that within the relevant speed ranges, bit rotation has a negligible effect on the flow of the water after it leaves the bit.

The calculations in Appendix C provide an explanation. For the water flowing out of holes on the face of the bit, the axial component of water velocity is much greater than the circumferential component. The ratio of velocity components is less for water flowing out of the flushing holes in the flutes. However these flushing holes are close to the wall of the hole but relatively far from the end of the hole. Thus any water moving outward from flushing holes in the flutes will impinge of the wall of the hole before flowing back along the annulus. Also, due to its greater diameter and rotational speed, outward flow from the flute flushing holes only occurred with the 48 mm diameter bit.

The results of the experimental and theoretical approaches were consistent. Hence the effect of bit rotation was judged to be insignificant and flow visualization with stationary bits in glass tubes was taken as valid.

Bit shown stationary.

Water from the face hole comes out in a stream, so it only covers the face of the bit when it is in a glass tube.

The water shown is all behind the face of the bit.

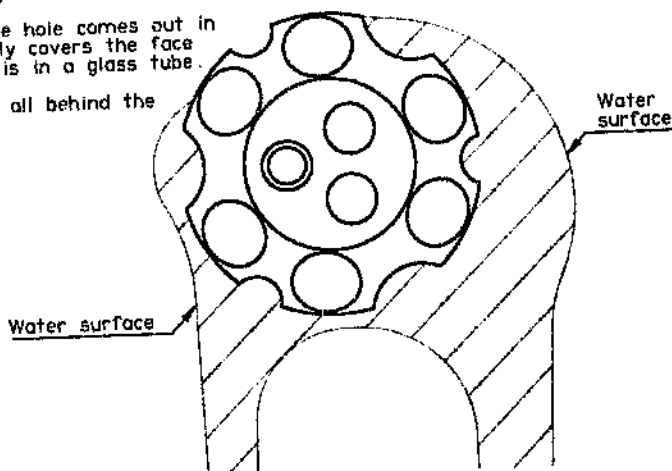


Figure 3.7 Outward flow from the flute flushing holes

### 3.5 FLOW/PRESSURE RELATIONSHIP

Since it is easier to measure than flow rate, the mining and drilling industries are normally only concerned about flushing water pressure. Thus, the flow/pressure relationship was investigated in order to:

- Relate these research results to industry practises.
- Make this research more useful.

The flow/pressure relationship was investigated separately from the drilling experiments, but the same rockdrills, bits and drill rods were used.

Water pressure at the inlet to the rockdrill was measured using an ordinary gauge. Flow rate was set and measured in the same way as for the drilling experiments.

## CHAPTER 4

### COMPUTER MODEL

#### 4.1 THE NECESSITY OF MODELLING

There are approximately fifteen commonly used sizes of button bits in the range from 32 to 215 mm diameter. Several different designs are available for each size and new designs are continuously being developed. All these sizes and each design in a particular size will have a different optimal flushing flow rate.

Despite its importance, information on optimal flushing flow rates is almost non-existent. Experimental work is time consuming and expensive. However, desktop and portable computers are widely used and suitable software is relatively cheap. Therefore, if a reliable, accurate computer model of the flushing process was available, it could be extensively used, for example in drawing offices where new bits are designed.

A computer model was developed to meet this need.

#### 4.2 OVERVIEW

The model simulates movement of a single chip from its formation near one of the buttons on the bit until it enters the annulus between the outside of the bit and the side of the hole. As shown in figure 4.1, it uses nested loops and iteration.

Starting from an initial low flushing flow the outer loop increases the flow rate until the chip reaches the annulus in the time between hammer blows. Each cycle through the inner loop calculates how far the chip moves in a single short time step. Water velocity, chip velocity and acceleration are held constant for the duration of each step. Thus the inner loop uses chip position and the previous values of water velocity and

chip velocity, to update chip position. This in turn is an input to the calculation of water velocity, which is combined with chip velocity for calculating chip acceleration. Chip velocity and displacement are calculated from chip acceleration and the duration of the step.

At the end of each step the model compares the updated value of chip displacement with the distance from the chip's starting point to the annulus. If the chip has not yet reached the annulus it compares elapsed time since chip movement started with the time between hammer blows. If either elapsed time or chip displacement are too big the outer loop increases the flow rate and the process is repeated.

The model predicts the minimum flow rate required to flush a chip of a defined size and shape from a given radial position to the annulus. It only simulates chip movement in the space between the end of the bit and the end of the hole. It does not include flushing in the annulus between the drill rods and the wall of the hole. This aspect of flushing is relatively well understood and if required, the model could be extended to include it.

#### 4.3 MODELLING PROCEDURE

Details of the modelling procedure, inputs and outputs are given in Appendix B, while the flow chart in figure 4.1 gives a graphic overview of the process.

In brief, the inner loop calculates:

- Water velocity at the chip;
- Force due to drag on the chip;
- Chip acceleration, resulting velocity and position at the end of the time step;
- Elapsed time.

The equations for each of these are presented in the form in which they are used in the model.

In the gap between the bit and the end of the hole the flushing water flows approximately radially outwards. Thus fluid velocity ( $v_f$ ) is

$$v_f = Q/A$$

where  $Q$  = volume flow rate  
 $A$  = effective cross sectional area at the radial distance corresponding to the position of the chip.

Effective cross sectional area ( $A$ ) was determined from the geometry of the bit and the resulting deviations from the assumed pattern of radial outwards flow.

Chip acceleration ( $a$ ) was calculated from the equation below for drag on a submerged body in subsonic flow [Douglas, Gasiorrek and Swaffield<sup>(16)</sup>].

$$a = \frac{C_d \cdot \rho \cdot A (v_f - v_c)^2}{2m}$$

where  $C_d$  = drag coefficient  
 $\rho$  = density of fluid (water)  
 $A$  = cross sectional area of the chip  
 $m$  = mass of the chip

Acceleration was assumed to be constant for each short time interval. Therefore the well known equations for constant acceleration straight line motion were used to calculate chip velocity and displacement.

$$v_c(n) = v_c(n-1) + a \cdot \Delta t$$

where  $v_c(n)$  = chip velocity for the current step  
 $n$  = step number  
 $v_c(n-1)$  = chip velocity for the previous step

a           = chip acceleration  
it          = duration of step

and

$$s(n) = s(n-1) \quad vc(n).it + \frac{1}{2}.a.it^2$$

where       s(n)     = chip position at the end of the  
                                current step  
             s(n-1) = chip position at the end of the  
                                previous step

Although the model simulates the movement of a single chip, the effect of other chips in reducing the cross sectional area available for fluid flow was taken into account.

Bit rotation was accounted for by assuming that the circumferential component of water velocity equalled half the angular velocity of the bit at the relevant radius (see section B2 in Appendix B for an explanation of the co-ordinate system). Chip motion was calculated in corresponding components and then combined to give resultant displacements.

#### 4.4       INPUTS AND OUTPUTS

Certain inputs have to be determined beforehand. These include:

- Chip sizes and masses (by measurement or estimation)
- Bit dimensions, from the drawings.
- The effect of the positions of the flushing holes and buttons on the flow across the end of the bit (see section B4 in Appendix B for details).
- Drilling parameters; most importantly percussion frequency.

Each run of the model ends when the flow rate is sufficient to flush the chip into the annulus in the time between hammer blows. This flow rate was then outputted.

Chips are formed at different positions and in a wide range of shapes and sizes. The highest flow rate outputted for a particular bit design, chip size and shape was taken as the predicted optimum for that combination. Multiple runs were therefore required. The results for various combinations of chip size and shape were combined for each bit size to create an overall picture.

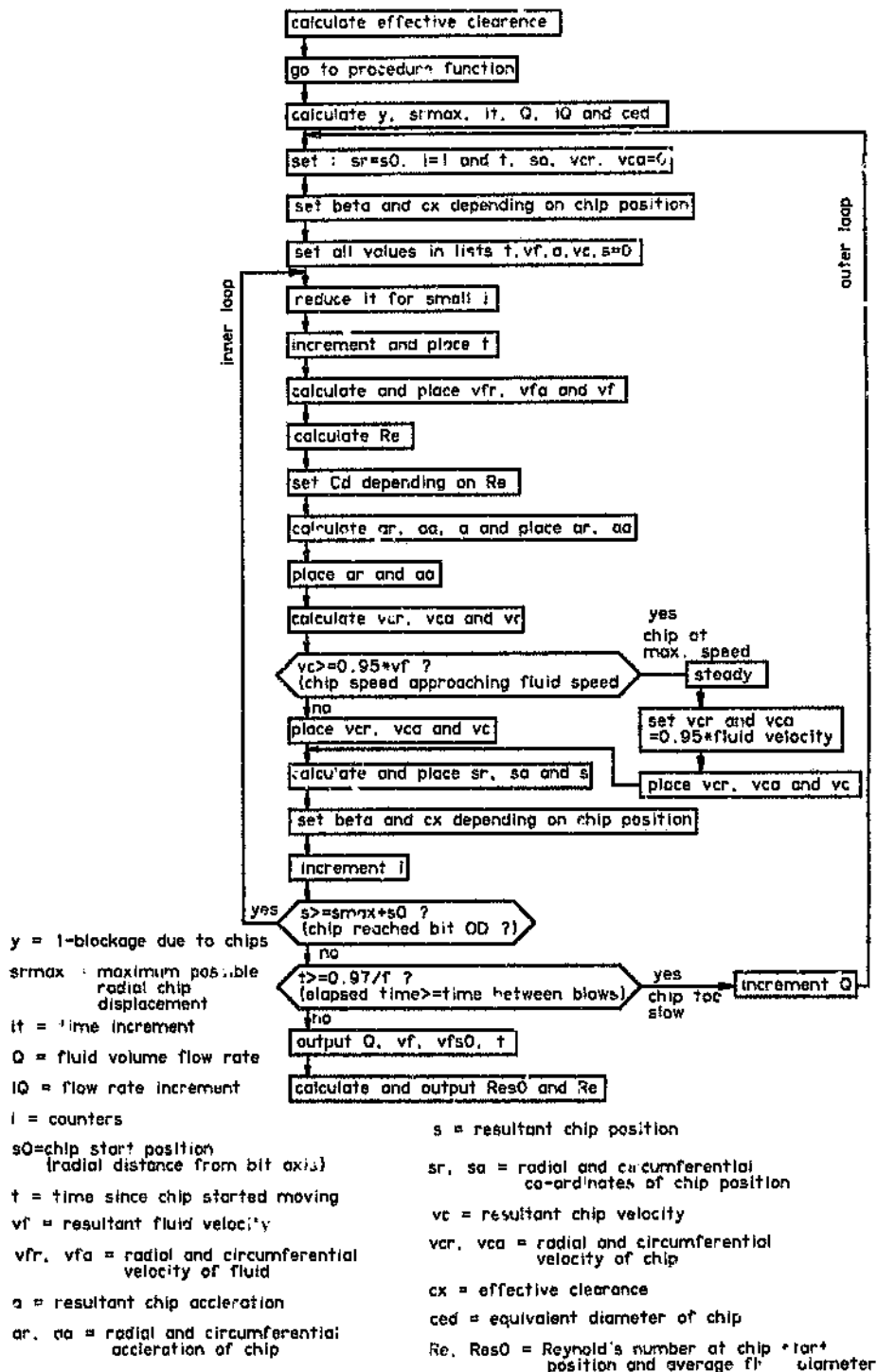


Figure 4.1 Flow chart for the computer model



## CHAPTER 5

### RESULTS AND DISCUSSION

From a commercial point of view the flow and pressure required to maximise penetration rate are most important. However, it is more logical to begin with the absolute minimum flow rate, below which drilling cannot proceed.

The data from the chip samples will be dealt with first because it explained some of the results and provided inputs to the computer model. Thereafter the data from the drilling experiments, computer modelling and flow visualization will be presented and discussed. Finally the results will be combined and synthesised into a unified whole.

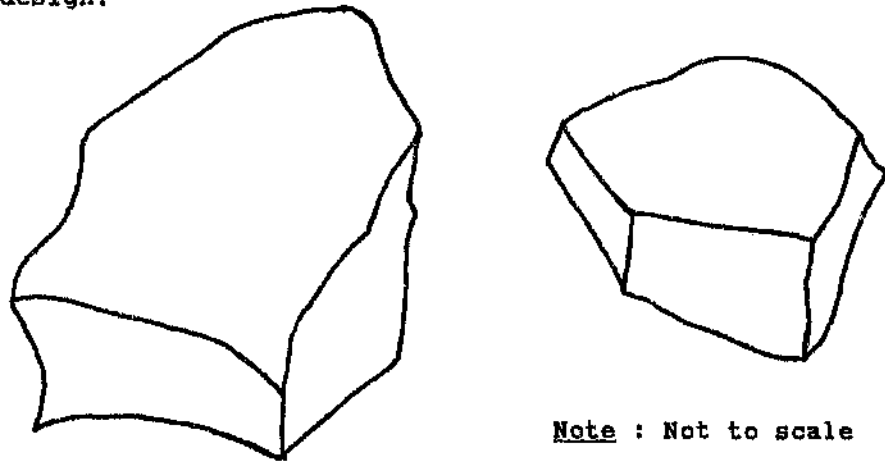
#### 5.1 CHIP SAMPLES

##### 5.1.1 SIZE, SHAPE AND SIZE DISTRIBUTION

The smallest of the sieves used for separating the chips into size fractions had a mesh size of 0.075 mm. Thus the dimensions of two sides of the chips in the smallest size fraction were less than 0.075 mm. When examined under an optical microscope these chips appeared close to equiaxed. For modelling purposes, they were assumed to be cubic with the length of any side equal to 0.05 mm, which gives a volume of  $1.25 \times 10^{-4} \text{ mm}^3$ . Since the density of quartzite is approximately  $2500 \text{ kg/m}^3$  [McFadzeal<sup>(5)</sup>], their mass was taken as  $3.125 \times 10^{-7} \text{ g}$ . They will henceforth be referred to as minute cubic chips.

Chips from the largest size fraction were usually flat and roughly rectangular (see figure 5.1). Therefore they will be referred to as large flat chips.

The average size of chips in the largest size fractions were dependant on the bit size. Chips collected from the 36 mm diameter bits drilling into concrete were significantly smaller than those produced by the by the 48 mm diameter bits drilling into rock. Although the shape of the largest chips from the two sources wa similar ie. flat and roughly rectangular (see figure 5.1), the chips obtained from the 36 mm diameter bits were thicker. Despite their much smaller size, these chips were about the same thickness as those obtained from the larger bits. It was not clear whether these differences were due to the materials being drilled and/or to the drilling process itself and/or to the bit design.



Note : Not to scale

Figure 5.1 Typical chip shapes

For both bits, as flow rate increased, the proportion (by mass) of large chips in the samples increased (see figure 5.2 and Appendix D). As explained in section 3.3, a simple heuristic approach was used for estimating the sizes of the chips in the largest size fraction.

Consider first the chips produced by drilling horizontally into quartzite rock with a 48 mm diameter bit and a hydraulic rockdrill. Typical sizes for the very largest chips (averaged from a number of chips) were:

Length - 9.3 mm  
 Width - 6.1 mm  
 Thickness - 2.7 mm

The maximum possible volume for very large flat chips was obtained by multiplying these dimensions together. However, due to the irregular shape of the chips, actual volume was taken as about half the maximum possible volume. The same procedure was used to estimate cross sectional area for the most likely chip orientation - ie. broadside on (see section 2.3). Mass was calculated from the estimated volume and the density of quartzite (approximately  $2500 \text{ kg/m}^3$  [McFadzean<sup>(5)</sup>]). Thus for large chips the figures in table 5.1 were used as inputs to the computer model.

Table 5.1 Properties of large chips

	48 mm diameter bit		36 mm diameter bit	
	Very largest chips	Average large chips	Very largest chips	Average large chips
Volume ( $\text{mm}^3$ )	76	9.6	38	6.4
Cross sectional area ( $\text{mm}^2$ )	39	4.9	19.7	3.3
Mass (g)	0.2	0.024	0.095	0.016

The average mass of the chips caught in the coarsest mesh (2.00 mm) was measured. It was taken as the mass of an average large flat chip and combined with the density of quartzite to determine volume. The procedure used for the very large chips was applied in reverse to get cross sectional area from the calculated volume. The resulting figures (see table 5.1) were used in the computer model.

Twelve samples were taken from the holes in the concrete block. These were drilled using 36 mm diameter bits and a pneumatic rockdrill. Typical sizes for the largest chips (averaged from a number of chips) were:

Length        - 5.9 mm  
Width         - 4.8 mm  
Thickness    - 2.7 mm

The procedure developed for the large chips from the 48 mm diameter bits also was applied to the chip samples produced by the smaller bits. Table 5.1 gives the resulting inputs to the computer model for the very largest chips and average large chips.

Since the computer model uses chip data to predict optimum flushing flow rates, the methods used for estimating chip size may not seem ideal. However, the predictions are not very sensitive to chip size. For example for average and very large flat chips the model for the 48 mm diameter bit predicts optimum flows of 14.693 and 15.057 l/min. The ratio of chip sizes is much bigger than the ratio of the predicted flow rates. Thus any small inaccuracies in the estimates of chip size have an insignificant effect.

As shown in figure 5.2, there was a correlation between the size distribution of the chips and the flushing flow rate (see also Appendix D for detailed data). Increasing flushing flow rate resulted in an increasing proportion (by mass) of large chips.

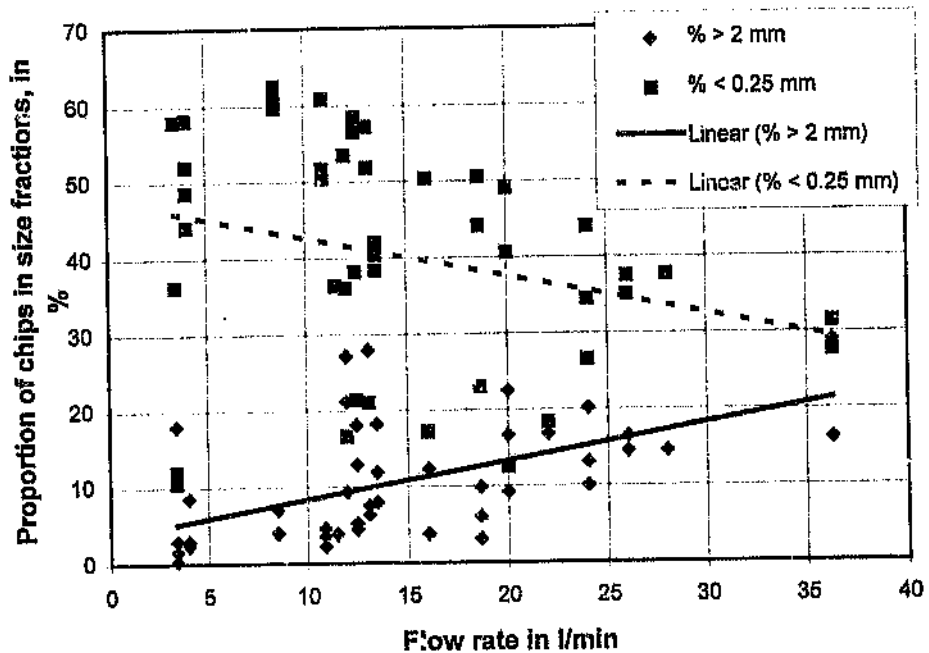


Figure 5.2 Effect of flow rate on chip size

Chip samples from both bit sizes confirmed and reinforced the observation of numerous previous researchers that adequate flushing results in bigger chips. The data also support their conclusions that:

- Inadequate flushing results in chips remaining too long in the space between the bit and the end of the hole. This excessive residence time leads to regrinding of the chips.
- If flushing flow is insufficient, the energy wasted in breaking chips after they are formed causes reduced penetration rates.

## 5.1.2 IMPLICATIONS OF SIZE DISTRIBUTION

Rock chips are irregularly shaped, but they can be represented by equivalent spherical chips. These have the same volume ( $V$ ) as real chips, therefore

$$V = (4.\pi.r^3)/3 \quad (1)$$

where  $\pi$  = ratio of the circumference of a circle to its diameter = 3.1416...

$r$  = radius of a spherical chip with volume equal to that of a typical non-spherical chip

and surface area ( $A_s$ ) is

$$A_s = 4.\pi.r^2 \quad (2)$$

The volume of a single hole ( $V_h$ ) is

$$V_h = \pi.D^2.l/4 \quad (3)$$

where  $D$  = diameter of hole drilled by button bit  
 $l$  = hole length

The volume of the hole equals the total volume of the chips formed while drilling the hole, therefore

$$V_h = (4.n.\pi.r^3)/3 \quad (4)$$

where  $n$  = the number of chips produced from the hole

so,

$$n = (3.V_h)/(4.\pi.r^3) \quad (5)$$

and the total surface area ( $A_t$ ) of the chips is

$$A_t = 4.n.\pi.r^2 \quad (6)$$

When rock is broken, the resulting creation of new surfaces requires energy. Assuming that losses are zero, (ie. efficiency = 100 %), all the percussion energy from the rockdrill goes into breaking rock at the end of the hole. Thus for a single hole

$$E = k.A_t \quad (7)$$

where  $E$  = percussion energy input to the hole  
 $k$  = energy required to create unit area of new surface

Combining equation 6 with equation 7 gives

$$E = 4.k.n.\pi.r^2 \quad (8)$$

Substituting equation 5 into equation 8 and simplifying gives

$$E = (3.k.V_h)/r \quad (9)$$

Substituting equation 3 into equation 9 and simplifying gives

$$E = (3.k.\pi.D^2/4)(1/r) \quad (10)$$

If everything except percussion energy input ( $E$ ) and average chip size ( $r$ ) are constant, then percussion energy input and average chip size are inversely proportional to each other. Thus if bit design was improved so that average chip size increased by say 10 %, then the percussion energy required to drill an identical hole would decrease by 10 %. This shows the importance of good bit design.

The only quantities in equation 10 which vary with time ( $t$ ) are percussion energy ( $E$ ) and hole length ( $l$ ). So, differentiating with respect to drilling time ( $t$ ) gives

$$\frac{dE}{dt} = \frac{(3.k.\pi.D^2/4r)(dl)}{(dt)} \quad (11)$$

Now  $dE/dt$  = percussion power input  
 $3.k.\pi.D^2/4r$  = constant  
 $dl/dt$  = penetration rate

Therefore, for constant average chip size, penetration rate is directly proportional to percussion power input to the rock.

Rewriting equation 11 gives

$$k = \frac{(dE/dt)(4r)}{3.k.\pi.D^2.(dl/dt)} \quad (12)$$

Equation 12 should be valid for brittle materials such as concrete and most types of rock. If so, it may provide a key to measuring the energy required to create unit area of new surface (k). When it was applied to the two different drilling situations researched, the resulting k values were as below (see Appendix C for calculations).

48 mm bit drilled into quartzite with a hydraulic rockdrill;  $k = 0.235 \text{ w/m}^2$

36 mm bit drilled into a concrete block with a pneumatic rockdrill;  $k = 0.079 \text{ w/m}^2$

The most likely reasons for the difference in the k values seem to be:

- Differences in the properties of the materials which the holes were drilled into.
- Enforced use (due to lack of better data) of percussion power output from the rockdrills instead of percussion power input to the bits. The two drill rod designs may not have the same energy transmission efficiency.



Further research along these lines may lead to useful insights about rock properties, the mechanism/s of rock breaking during drilling and the characteristics of drilling equipment.

Alternatively, if all the quantities on the right hand side (including the constant  $k$ ) are known or can be determined then equation 12 could be used in:

- Investigating how much of the percussion energy output from a rockdrill actually does useful work on the rock and how much is lost in transmission from the rockdrill to the end of the hole. This will also provide a measure of the energy transmission efficiency of drill rods and bits.
- Predicting average chip size, and comparing it with measured chip size. The difference will show how much regrinding has occurred.

If percussion power input ( $dE/dt$ ) is constant but average chip size ( $r$ ) varies, then penetration rate ( $dl/dt$ ) and average chip size ( $r$ ) must be directly proportional to each other - in symbols

$$r = \frac{(3.k.\pi.D^2)(dl)}{4(dE/dt)(dt)} \quad (13)$$

$$\text{and } \frac{3.k.\pi.D^2}{4(dE/dt)} = \text{constant}$$

Thus a 10 % increase in penetration rate should lead to a 10 % increase in average chip size. Figure 5.3 shows that as penetration rate increased the proportion of chips in the largest size fraction (greater than 2 mm) increased while the proportion of chips in the smallest two size fractions (less than 0.25 mm) decreased.

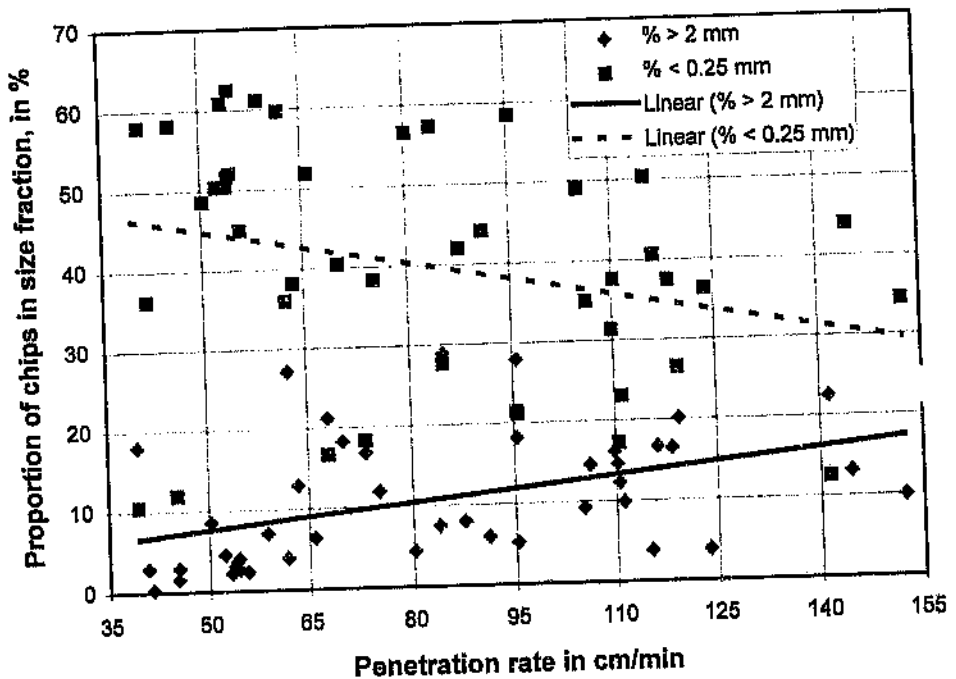


Figure 5.3 Effect of penetration rate on chip size

## 5.2 FLOW AND PENETRATION RATES

Figure 5.4 summarises the data for both drilling situations. In very broad terms it shows that as flushing flow is increased from a low value, penetration rate increases with increasing flow rate. Eventually penetration rate reaches a final plateau and further increases in flow do not seem to affect penetration. The kink in the graph before it finally levels out defines the optimum flushing flow rate. Berson<sup>(3)</sup> reported a similar trend.

The real situation is more complex than the ideal described above.

The curve for the 48 mm diameter bit has two plateaus - the first at relatively low flow and penetration rates and the second or final one at higher rates. Optimum flushing (minimum flow for maximum penetration rate) for the 48 mm bit is approximately 15 l/min - ie. at the kink defining the edge of the final plateau.

The curve for the 36 mm diameter bit only has one plateau. After a linear section, penetration rate peaks before dropping slightly. Thereafter the curve becomes horizontal and penetration rate appears to be independent of further increases in flow. Optimum flushing for the 36 mm diameter bit is the flow at which penetration rate is a maximum - ie. approximately 3.0 l/min.

The shapes of the curves will be explained in subsequent sections.

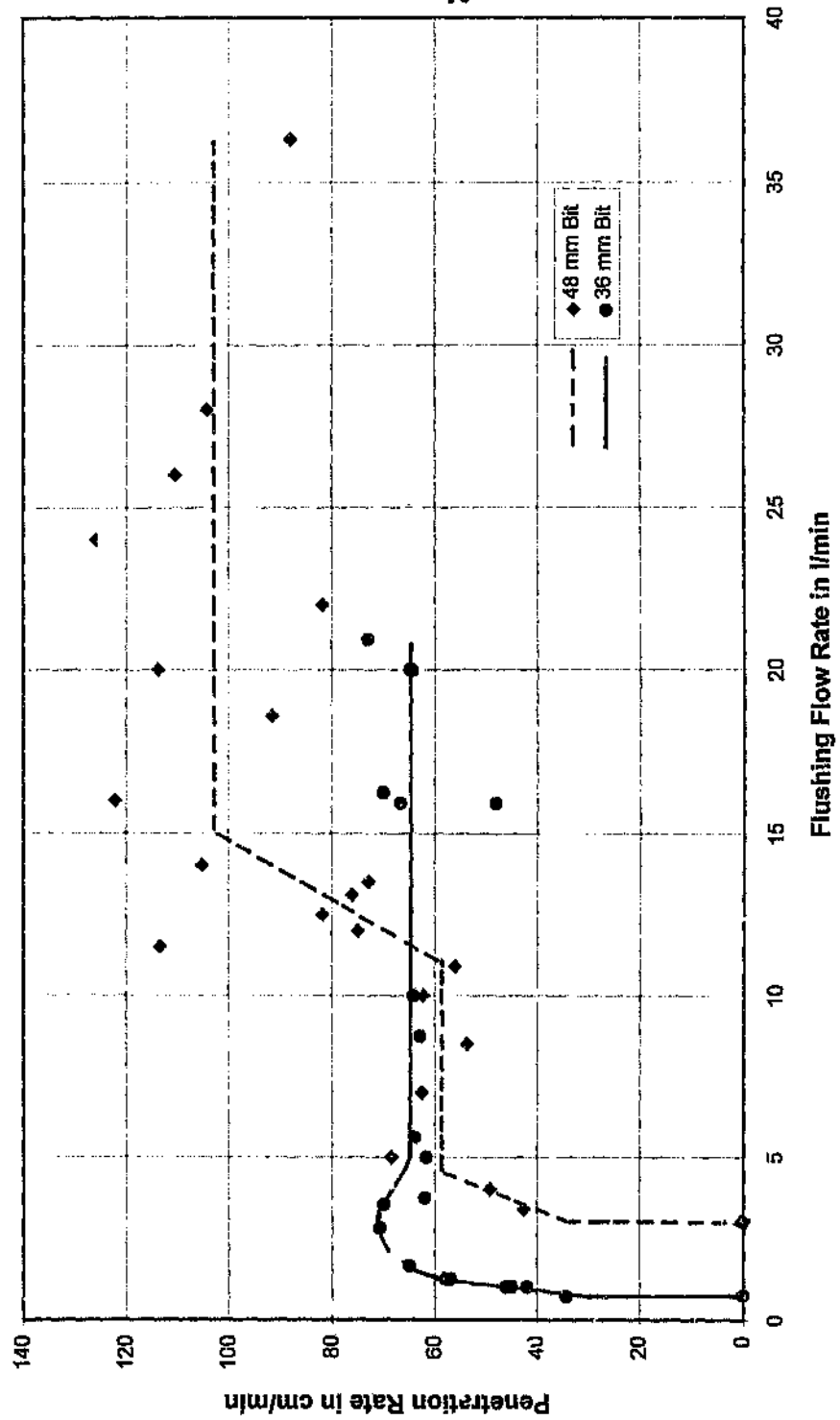


Figure 5.4 Effect of flow rate on penetration rate

### 5.2.1 ABSOLUTE MINIMUM FLOW RATE

In figure 5.4 the absolute minimum flushing flow rates are indicated by the points on the X axis.

Drilling with the 36 mm bit and pneumatic rockdrill into the concrete block proved beyond doubt that:

- An absolute minimum flushing flow rate exists.
- It is approximately 0.7 l/min, for this combination of drilling equipment.

Since penetration rate was maximised at a flow of about 3.0 l/min, absolute minimum flushing is significantly greater than zero.

A flow of 0.72 l/min. was just sufficient to complete a 1.05 m deep hole, but the bit and drill rod seized in the hole as full depth was attained. Normally removing the bit and rod from the hole takes a few seconds. However, after they stuck in the hole, two experienced drill operators needed about half an hour to remove them. Thus, allowing for a small safety margin, the minimum feasible flushing flow is approximately 0.8 l/min.

To avoid similar downtime on the hydraulic drill rig, no attempt was made to determine what the absolute minimum flow rate for the 48 mm bits was. Even if it were known exactly, it is of no practical value because cost effective drilling requires a very much higher flow rate. Based on the drilling data for flow rates below 5 l/min, the absolute minimum flushing flow for the 48 mm bit is probably near 3 l/min.

Considering these absolute minimum flow rates in relation to the optimum flows, it seems as if the absolute minima are approximately 1/4 to 1/5 of the optimums.

When flushing is sub-optimum chips remain in the space between the bit and the end of the hole for relatively long periods. Since their residence times are greater than the time between hammer blows they are reduced in size by regrinding (see section 5.2.2 for details). If regrinding is due to inadequate flushing then the extent of regrinding may be inversely proportional to flushing flow rate.

At flow rates lower than the absolute minimum, few chips are flushed out of the hole. Thus a thick slurry with a very high concentration of small reground chips fills the hole. Bits recovered from such conditions exhibit blockage of their face flushing holes by slurry. Therefore no or very little flushing fluid reaches the gap between the bit and the end of the hole. Thus the slurry there is even denser than that in the annulus between the drill rods and the wall of the hole. Penetration stops because the slurry at the end of the hole absorbs the drilling energy. At the same time, the slurry in the annulus prevents movement of the drill rod and bit.

If the rockdrill is not stopped immediately, the continuing input of energy without adequate means of removing it, results in heating of the bit and drill rod. This may be sufficient to turn some of the little water in the hole into steam. It also illustrates the importance of the secondary function of flushing fluid - i.e. removal of drilling energy from the hole as heat.

#### 5.2.2 EXPLANATION FOR PENETRATION AND FLOW DATA

Figure 5.4 shows that when drilling slightly downwards with a pneumatic rockdrill and 36 mm diameter bit:

- Above the absolute minimum flow, penetration rate increased linearly with increasing flow rate from 0.72 l/min up to about 1.6 l/min.

- At flows between 1.6 l/min and 3 l/min, penetration rate continued increasing but more slowly.
- Penetration rate peaked at a flushing flow of approximately 3 l/min.
- Thereafter penetration rate decreased slightly.
- At flushing flows greater than 5 l/min penetration rate remained constant irrespective of further increases in flow rate.
- Average penetration rate at flushing flow rates greater than 5 l/min was slightly lower than the peak penetration rate.

Flow visualization showed that complete coverage of the face of the bit occurs at between 2 and 2.1 l/min. Therefore, at flows below 2 l/min no flushing water reaches the upper part of the face of the bit. Thus there is no flushing of the top part of the end of the hole. Hence chips produced by buttons impacting there are not flushed out in the time between hammer blows. Their excessively long residence time in the space between the end of the bit leads to regrinding. Penetration rate is reduced because percussive energy is absorbed in regrinding.

Assuming this reasoning is correct then it is possible that the inflexion point at about 1.6 l/min may be due to a change in the nature of the flow over the bit. If so, then the results of the flow visualization explain the change in slope.

The computer model for the 36 mm diameter bit explains the next part of the curve, including why 3 l/min is optimum. The model predicts the flow required to flush a chip, within the time between hammer blows, from wherever it is formed on the end of the hole into the annulus between the bit and the side of the hole.

Inputting the characteristics for minute cubic chips (see section 5.1.1) into the computer model resulted in a prediction that a flow of 2.749 l/min is sufficient to flush such chips into the annulus in the time between hammer blows (see table D4).

The results for very large flat and typical large flat chips (see section 5.1.1) were identical to each other. When the characteristics of these chips were inputted into the model it predicted that a flow rate of 3.307 l/min was sufficient to flush them from where they were formed into the annulus in the time between hammer blows. Thus the model's prediction was within 11 % of the experimental observation (3 l/min).

The model also showed that small chips require lower flows for adequate flushing. Hence at 3.307 l/min all chips would have been flushed into the annulus in the time between hammer blows. Thus no percussion power would be wasted in regrinding and further increases in flow could not increase flow rate.

The observed drop in penetration rate after it peaked at just over 70 cm/min was due to failure of the drill rod. When a drill rod breaks penetration rate drops but it is not immediately noticeable - even to the most experienced and alert of rockdrill operators. Hence the recorded time for that particular hole was probably about ten seconds longer than the actual drilling time. Since penetration rate was calculated on the recorded time rather than actual time, it was somewhat lower than it should have been.

Small pneumatic rockdrills (such as that used for this research) have their connection point for the flushing fluid supply hose on the back end of the rockdrill (see figure 5.5). A long thin tube is provided to take the fluid from the connection point to the drill rod. Due to



the length and diameter of the tube the maximum flushing flow which can be passed through the rockdrill is severely limited. Once the flow is significantly greater than 5 l/min the pressure drop is so great that it is very difficult to keep the supply hose attached to the rockdrill.

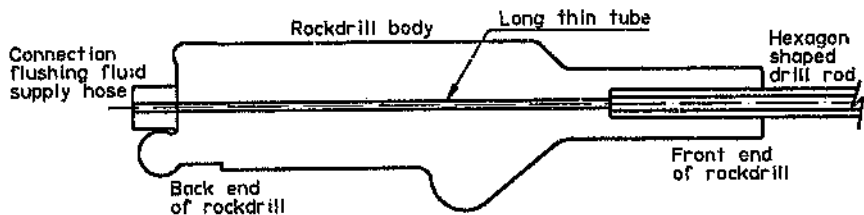
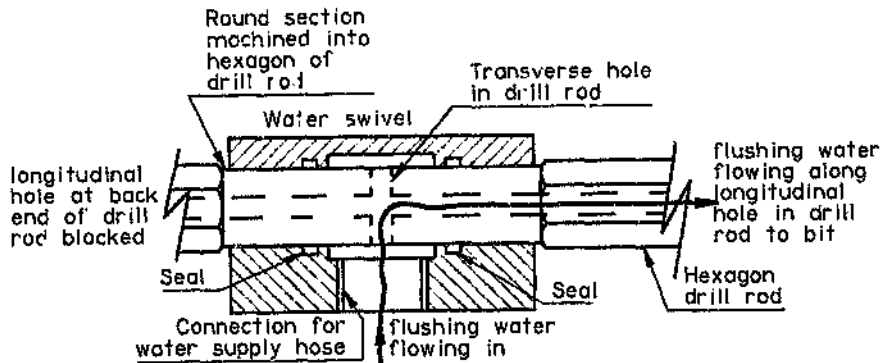


Figure 5.5 Flushing fluid passage through the pneumatic rockdrill

A modification was made to overcome this constraint and allow drilling at flushing flows greater than 5 l/min. Instead of sending the flushing fluid to the drill rod via the rockdrill, a more direct route was used. As shown in figure 5.6 a round section was machined into the hexagon shaped drill rod, two transverse holes were added and the back end of the drill rod was blocked. A water swivel was then attached to the drill rod and the supply hose was connected to the water swivel. Thus flow was through the water swivel and then into the drill rod.

Without this change to the equipment no drilling could have been done at flushing flows much above 5 l/min. Unfortunately the change affected the results of the drilling experiments with the 36 mm diameter bits. The lower average penetration rate at flows above 5 l/min was probably caused by the reduced percussion energy transmission efficiency of the modified drill rod.



Note : Some detail omitted

**Figure 5.6 Modification to the equipment for the 36 mm diameter bit**

Longitudinal impact waves travelling through metal are reflected off free surfaces [Timoshenko<sup>(17)</sup>]. When the drill rod was modified for the water swivel additional free surfaces were machined into it. Some of the energy from the rockdrill would have been reflected off these free surfaces and thereby lost. Thus penetration rate decreased slightly when the modified rod was used.

The scatter in penetration rate at flows above 5 l/min was probably mostly due to variations in the concrete and/or the air supply pressure to the rockdrill.

For the 48 mm diameter bits, figure 5.4 shows four distinct regimes above the absolute minimum flow rate:

- Penetration rate increasing with flow rate up to about 5 l/min.
- Constant or slowly increasing penetration rate at flow rates between 5 and 11 l/min.
- Penetration rate increasing rapidly but irregularly at flows between 11 and 15 l/min.
- Constant or slowly declining penetration rate at flows above 15 l/min.

It can be inferred from the flow visualization that low flow rates provided too little water to completely cover the face of the bit and the end of the hole. Thus it is possible that there was a free surface of water between the end of the bit and the end of the hole. Figures 5.7 and 5.8 are a record of the observations during flow visualization. They show how the position of the free surface varied with bit orientation and flow rate.

At 3.8 l/min on average only about 80 % of the face of the bit and the end of the hole might have been covered by flushing water. If so, no flushing water would reach the upper part of the hole. However, transmission of percussion from the bit to the rock is independent of flushing. Therefore buttons impacting on unflushed parts of the end of the hole still create new chips. If the flow visualization is correct then these chips will be formed above the free surface of water. Thus they first have to fall into the flushing water under gravity before they can be flushed into the annulus.

The percussion mechanism of the rockdrill was running at 49 Hz and each percussive impact has a very brief but finite duration. The time between impacts was less than 0.02 seconds. As shown in Appendix C, the maximum distance which chips could move under gravity in this time was 3.8 mm.

As shown in figure 5.7 the distance from the free surface to the periphery of the bit can be greater than 3.8 mm. Thus any chips formed on the unflushed upper part of the end of the hole will have excessively long residence times. In other words, due to the short time between hammer blows, chips formed above the free surface of water in the hole will still be between the end of the hole and the face of the bit for the duration of the next few percussion cycles. Their presence there will result in some of the energy of successive impacts being

absorbed in regrinding chips formed during previous cycles. Thus if flushing water does not cover the end of the bit and hole completely, penetration rate will be reduced.

As the flow rate increased, the size of the unflushed part of the end of the hole decreased. Figure 5.8 shows that at a flow of 4.8 l/min. on average, only about 10 % of the end of the bit and the hole may have remained unflushed. This is consistent with the experimental observation that penetration rate increases as flow increases.

Flow visualization also suggested that at about 5.5 l/min the end of the hole was fully covered by flushing water in all bit orientations. Thus this mechanism could not produce further increases in penetration rate. This seems to account for the levelling out of the curve for the 48 mm diameter bits to form the first plateau in figure 5.4. Small fluctuations in the experimental data were probably due to variations in the rock.

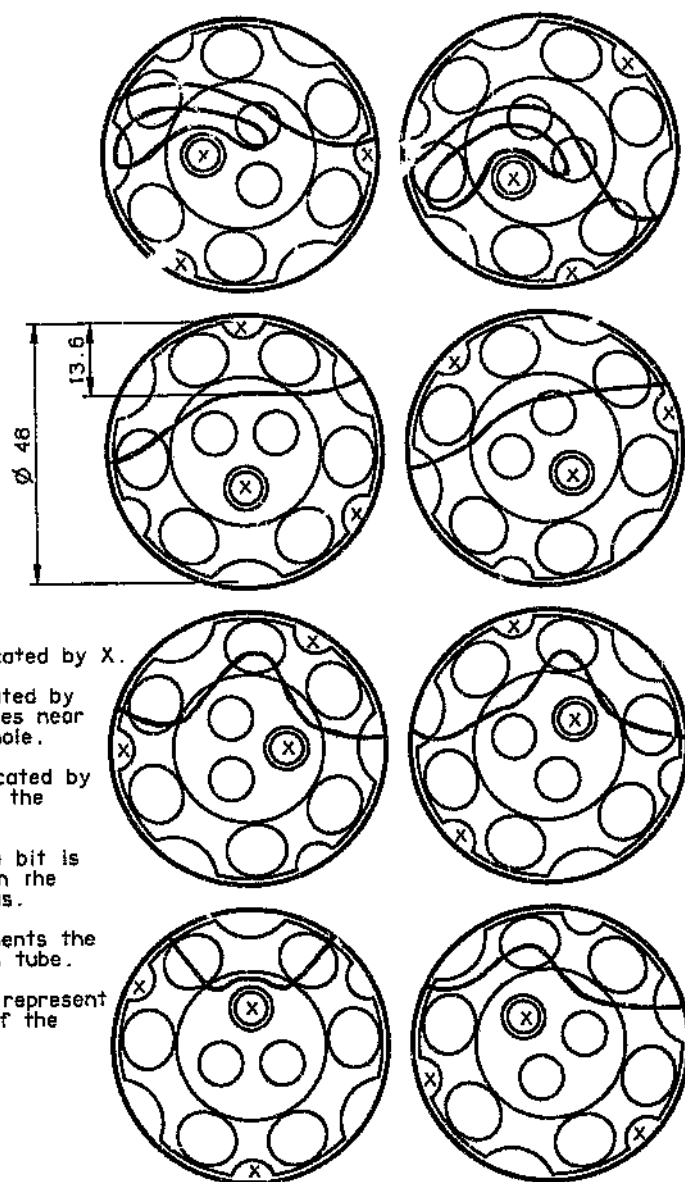


Figure 5.7 Fluid coverage at 3.9 l/min.

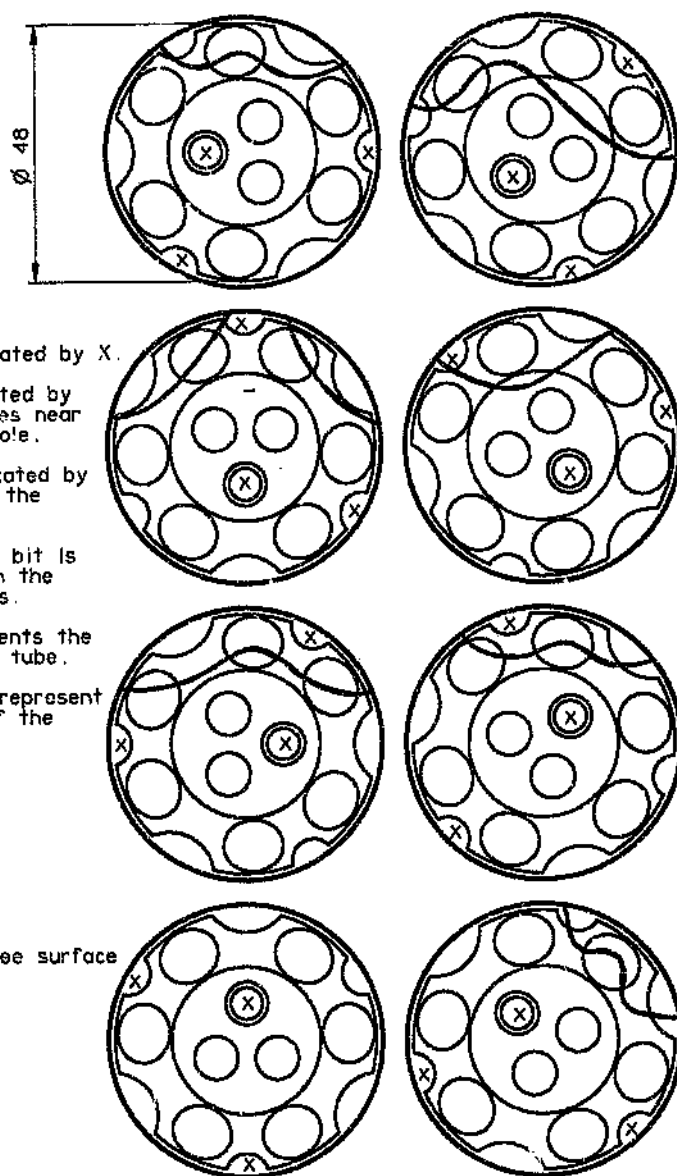


Figure 5.8 Fluid coverage at 4.8 l/min.

The computer model for the 48 mm diameter bit was run with inputs for a minute cubic chip and two sizes of large flat chips (see section 5.1.1). Figure 5.9 is a particular representation of the results. The peaks of the curves show the maximum flow rate needed to flush the various chips into the annulus in the time between hammer blows. Since they are the critical or worst cases these flow rates are used in the subsequent discussion. Figure 5.9 a' shows that the predictions for the two sizes of large chips are very similar. Thus correct estimation of chip size is not vital - even relatively large error in estimation should not lead to significant errors in the model's predictions.

For minute cubic chips the model predicted that a flow of 10.491 l/min is needed to flush all chips of this size and shape into the annulus in the time between hammer blows (see table D3). Figure 5.4 shows a sudden change at approximately 11 l/min, therefore the model's prediction is within 1 % of the experimental observation.

When the characteristics of the large flat chips (see section 5.1.1) were inputted into the model, it predicted that:

- A flow of about 15.1 l/min is needed to flush the very largest chips into the annulus between the bit blows.
- Large flat chips at a radial position of 9 to 9.5 mm required the highest flushing flow (see section 5.4 for explanation).

The experimental results show that a flow of about 15 l/min was sufficient to maximise penetration rate. The model's prediction was within 1 % of the experimental observation.

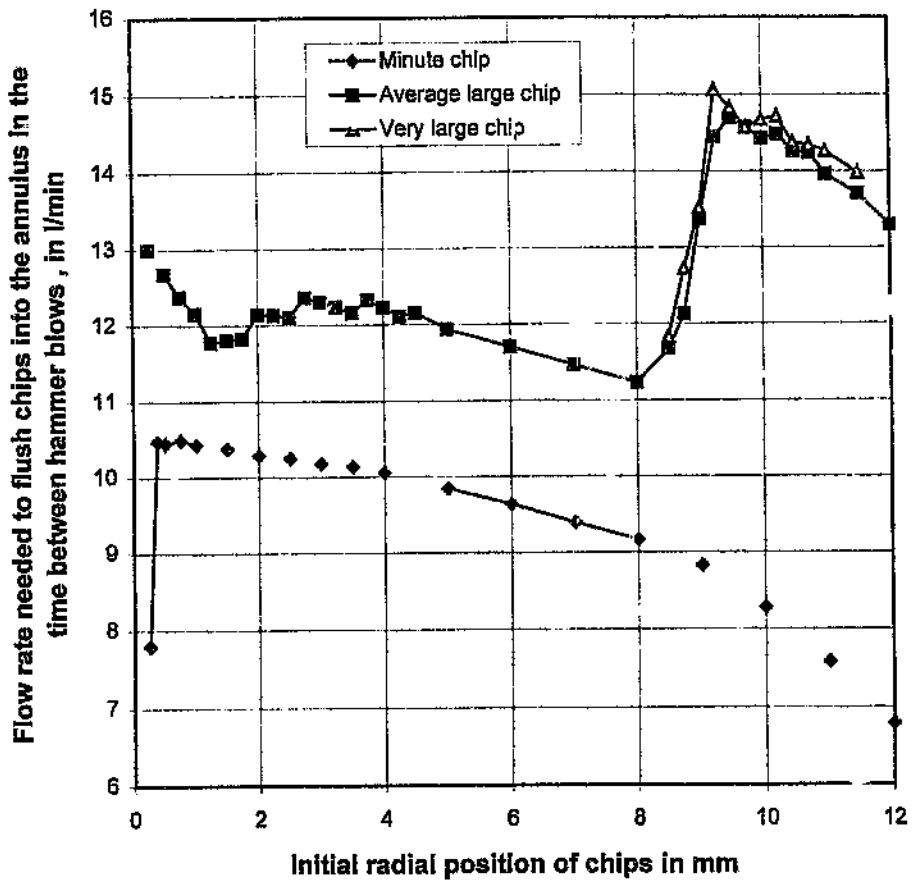


Figure 5.9 Flushing of different sized chips

The close correlation of the theoretical and experimental results indicates that after flow was sufficient to cover the end of the hole, penetration rate could only increase once the smallest chips started being flushed out in the time between hammer blows. Once the flow rate was sufficient to flush all the chips (including the very largest ones) into the annulus in the time between hammer blows, further increases in flow rate could not increase penetration rate.



In conclusion, all evidence seems to indicate that:

- At low flushing flow rates increasing fluid coverage of the face of the bit and the end of the hole increases penetration rate.
- If flow rate continues increasing, beyond the point at which full coverage has occurred, eventually the smallest chips are flushed into the annulus in the time between hammer blows.
- Penetration rate then increases with increasing flow because progressively more of the larger chips are being flushed out in the time between hammer blows.
- Once all sizes of chips are flushed out in the time between hammer blows no further increases in penetration rate are possible.

Chip size and drilling energy are keys to understanding the mechanism whereby penetration rate varies at higher flow rates. The drilling energy input to the rock can go into creating new rock surfaces or into heat due to rubbing of the bit on the rock. New surfaces can only be created by:

- Forming new chips on the end of the hole, which is useful because it deepens the hole. It was measured as penetration rate.
- Breaking down (regrinding) already formed chips. Energy consumed on regrinding is wasted because it does not contribute to penetration.

Regrinding with commensurate loss of drilling energy can only occur due to contact between chips and the drill bit or drill rod. The gap between the end of the bit and the end of the hole is much smaller than the gap in the annulus between the drill rod and the sides of the hole. Therefore most of the energy loss must occur in the gap between the end of the hole and the bit. Berson<sup>(4)</sup> has shown that most regrinding happens there.

Almost all drilling energy is in the percussion (ie. stress waves) rather than rotation of the drill rods and bit. Percussion energy loss due to regrinding can only occur at the time the hammer blow is being transmitted from the bit to the rock. Hence, only chips which are between the end of the bit and the end of the hole can absorb drilling energy by being reground.

Thus, the logical conclusion is that as soon as the concentration of chips at the end of the hole decreases the penetration rate will increase. The results from the computer model and all experimental data (chip sample , flow visualization and drilling) combine to support the conclusion.

At flows above the optimum (3.0 l/min for the 36 mm diameter bits and 15 l/min for the 48 mm diameter bits) all the chips should be flushed out from the space between the face of the bit and the end of the hole in the time between hammer blows. Thus, additional flushing flow cannot increase penetration rate and it remains constant.

### 5.3 FLOW RATE AND SCATTER IN PENETRATION RATE DATA

Figure 5.10 shows that for the 48 mm diameter bit, as flow increased the variation in the penetration rate also increased (The line was produced by least squares linear regression). The data seem to imply that at low flow rates where flushing was inadequate, flushing was the dominant mechanism in limiting penetration rate. As flushing improved with increasing flow, the dominant mechanism in limiting penetration rate changed to the rock properties.

In the North Pit at West Wits, where the 36 mm diameter bits were drilled, the rock strata (layers) are predominantly horizontal. To reduce the influence of



#### 5.4 INITIAL CHIP POSITION AND FLOW RATE

The data in figure 5.9 was obtained from the computer model. It indicates that for the 48 mm diameter bit :

- There is a definite relationship between the position at which a chip is formed and the flow rate needed to flush it out in the time between hammer blows.
- For minute cubic chips, the position at which maximum flow is required is near the centre of the bit whereas for large flat chips it is much further away.

When chips are formed their velocity is zero. Drag from the water moving past them results in the chips accelerating so that their velocity tends towards that of the flushing water (see figure 5.11). But chip velocity is limited by the velocity of the flushing water (see section B8 in Appendix B for detailed explanation). Since the water velocity is declining, chips which accelerate fast enough for their velocity to approach that of the fluid will then decelerate as fluid velocity decreases.

Consider the motion of two identical chips formed at different radial positions (see figure 5.11). Close to the centre of the bit, water velocity is high, therefore the chip formed here accelerates rapidly to a relatively high speed. However, the chip has to travel a long way before it reaches the annulus. Conversely, near the outside of the bit, water velocity is much lower, so the chip formed here accelerates more slowly to a lower speed. Nevertheless it does not have to travel as far as chips closer to the centre of the hole.

These two effects (declining acceleration and declining distance) together determine which radial position will require the highest flow.

Large flat chips which accelerate relatively slowly have a lower average velocity. Thus for them to be flushed into the annulus in the time between hammer blows they have to travel a shorter distance. Therefore their maximum flow position is relatively far from the centre of the bit. On the other hand, minute cubic chips accelerate much faster than large flat chips (see figure D5). Hence their average velocity is much higher and their maximum flow position is close to the centre of the bit.

Figure 5.11 shows how the velocity of the water and of an average large flat chip varies with radial position across the face of the 48 mm diameter bit. The solid lines are for a chip formed 8 mm from the centre of the bit and the dotted lines are for a chip formed 9.5 mm from the centre of the bit ( $s_0$  = initial radial position of the chip). These initial chip positions were chosen because the model predicts a big increase in required flow rate between these two positions (see figure 5.9). The water velocity curves are for the flow rates required to flush chips formed at the two different initial positions into the annulus in the time between hammer blows. An average large flat chip formed at 9.5 mm needs a higher flow than an identical chip formed at 8 mm, therefore the velocity curves are displaced corresponding to the velocity of the flow required to flush each chip into the annulus in the time between hammer blows.

The changes in water velocity at radial positions of about 8, 14 and 17 mm are due to changes in the cross sectional area available for flow. The face of the bit was split into five concentric annular areas or rings (see section B4 in Appendix B). At any radius, cross sectional area for flow was calculated from button protrusion, circumference and blockage due to the buttons. X2 to X5 in figure 5.11 indicate the proportions of the area remaining after taking blockage into account.

Figure 5.11 shows that at a radial position of 8 mm water velocity is relatively high (greater than 2 m/s), therefore chips formed there are accelerated rapidly. At a radius of 9.5 mm water velocity is much lower (approximately 1.25 m/s) thus chips formed there accelerate relatively slowly. Despite the chip formed at 9.5 mm being flushed out by higher velocity water, its velocity only exceeds that of the other chip at a radial position of about 14.5 mm. Even then the velocity of the chip formed further out never exceeds that of the other chip by very much. The higher initial acceleration of the chip formed at 8 mm is sufficient for it to require a significantly lower flow rate for it to be flushed into the annulus in the time between hammer blows.

Enrik and Klinzing<sup>(18)</sup> found that for pneumatic conveying the length of pipe required to get particles to constant speed is directly proportional to particle diameter to the power of 1.26. Therefore in a compressed air stream, small particles accelerate much faster than larger ones. The behaviour of rock chips in flushing water seems to be similar.

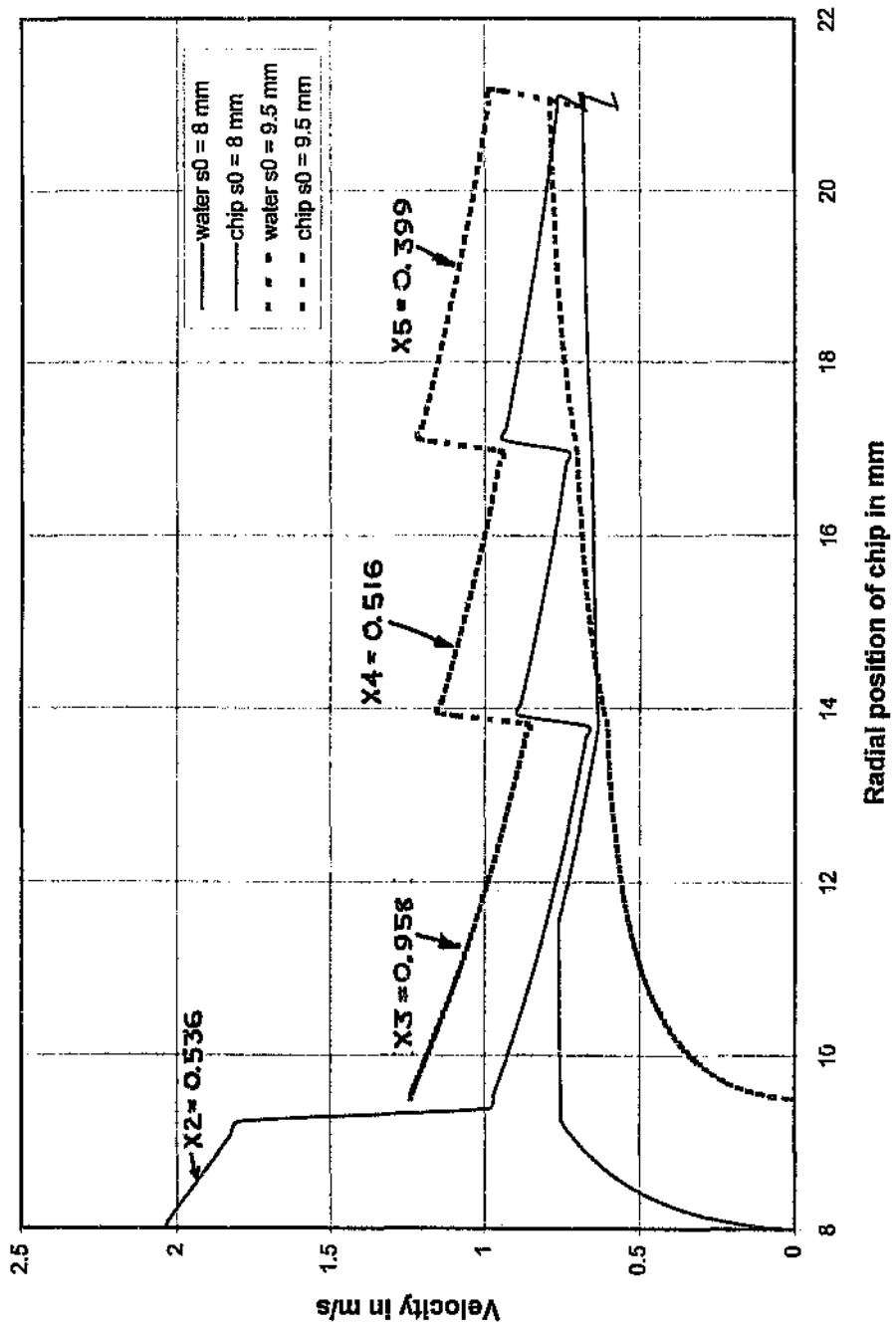


Figure 5.11 Chip and fluid velocities

### 5.5 FLOSHING WATER PRESSURE

Whether or not flushing is adequate depends on flow rate. Pressure is dependent on the resistance to flow through the rockdrill, drill rod/s and bit.

Experimentation with the pneumatic rockdrill, drill rod and 36 mm diameter bit showed that a water supply pressure of 170 kPa was required for a flow rate of 1.58 l/min. The pressure drop through pipes, fittings and orifices increases with the square of flow rate [Daugherty and Franzini<sup>(19)</sup>]. Therefore, at the optimal flow rate of 3 l/min a supply pressure of  $170 \times (3/1.58)^2 = 613$  kPa is required. This is close to the top end of the range of pressures normally available in South Africa for drilling 36 mm diameter bits with pneumatic rockdrills [Loots<sup>(10)</sup>]. Hence, in many South African mines the flushing flow to pneumatic rockdrills using 36 mm bits is probably less than optimal. If so, penetration rates will be lower than they could otherwise be.

However, over a relatively wide range of flows around the optimum, penetration rate is not very sensitive to changes in flushing. For example, if supply pressure doubles, the quadratic relationship between flow and pressure results in a flow rate increase of only  $\sqrt{2}$  times (1.41 times or 41 %). Figure 5.4 shows that for a 36 mm diameter bit, increasing the flow rate from 2 to 3 l/min. (50 %) only increases penetration rate by about 10 %. Thus, over a limited range of flows, sub-optimal flushing may not noticeably reduce penetration rate. However, due to the shape of the curve, a large decrease in supply pressure will have a very significant effects on penetration rate.

The data plotted in figure 5.12 were obtained at West Wits. Thus the curve is strictly only applicable to the 48 mm diameter bits and hydraulic rockdrill used there



(see Appendix A for details). Nevertheless it indicates that a water supply pressure in the range 200 to 250 kPa is likely to be sufficient to produce optimum flushing (15 l/min.) for a 48 mm diameter bit. Water supply pressures of 1500 to 1800 kPa are common in similar applications [Schwartz<sup>(8)</sup> and Brewitt<sup>(9)</sup>]. Therefore, in these cases the flushing flow is probably way above the minimum required to maximise penetration rate.

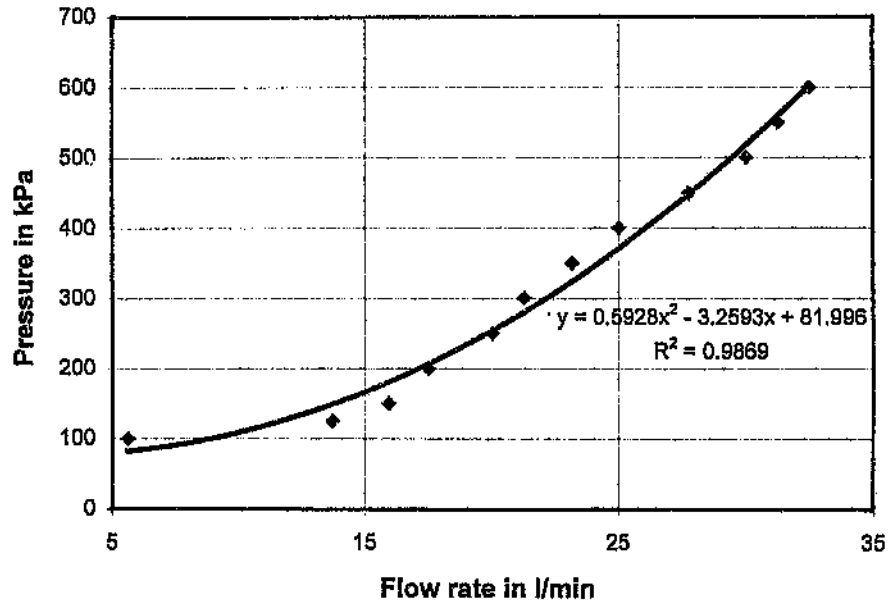


Figure 5.12 Water pressure

## CHAPTER 6

### CONCLUSIONS

- 6.1 Efficient rotary percussion drilling with button bits depends on flushing the chips formed by each hammer blow out of the gap between the bit and the end of the hole in the time between hammer blows.
- 6.2 A minimum flushing flow rate is required to maximise penetration rate. Using a higher flow rate will not produce an increased penetration rate.
- 6.3 If flushing is insufficient some chips remain in the gap between the bit and the end of the hole for longer than the time between hammer blows. In this position they are reduced in size (reground) by subsequent hammer blows.
- 6.4 Regrinding absorbs some of the energy which should go into deepening the hole, thereby reducing penetration rate. It also results in the chips collected from holes drilled with inadequate flushing being smaller on average than those collected from holes drilled with sufficient flushing flow.
- 6.5 There is a non-zero absolute minimum flushing flow rate below which drilling is impossible. For 36 mm and 48 mm diameter bits the absolute minima are approximately 0.8 and 3 l/min respectively. These absolute minima appear to be between 1/4 and 1/5 of the optimum flow rates.
- 6.6 In horizontal holes a certain minimum flow rate is needed to completely cover the end of the bit with flushing water. This flow rate is considerably lower than the optimal rate.

- 6.7 Percussion energy input and average chip size are inversely proportional. Since average chip size is partly a function of bit design, optimising bit design can reduce the drilling energy requirements.
- 6.8 Chip sample and drilling data may provide a means of determining the energy needed to create unit area of new rock surface.
- 6.9 For a hydraulic rockdrill and 48 mm diameter bits in horizontal holes a water flow of about 15 l/min is sufficient to maximise penetration rate.
- 6.10 For a pneumatic rockdrill and 36 mm diameter bits in almost horizontal holes a water flow of about 3.0 l/min is sufficient to maximise penetration rate.
- 6.11 Flushing can be modelled by calculating the forces on a single chip and thereby determining the water flow rate required to flush it into the annulus between the bit and the sides of the hole in the time between hammer blows.
- 6.12 The computer model was able to predict the optimum flushing flow rates for two of the most widely used sizes of button bit to within 10 %.
- 6.13 All important features on the curves of penetration rate against flow rate can be explained by combining chip sample data, observation of the flow over the bit and the predictions of the computer model.
- 6.14 The computer model also showed that:
  - 6.14.1 Small chips require a lower flushing flow rate than larger ones.
  - 6.14.2 The position at which a chip is formed affects the flushing flow which it needs.
  - 6.14.3 Large chips formed near the centre of the bit require less flushing flow than identical chips formed further out.

## CHAPTER 7

### SUGGESTIONS FOR FURTHER WORK

- 7.1 The research might be repeated for other sizes and designs of bit.
- 7.2 Although water is the most common flushing medium, compressed air and multiphase mixtures such as air plus water, air, water plus foam are also used. The computer model could be adapted to handle some of these other fluids, especially compressed air, since it is the second most used flushing medium. The predictions of any new or extended computer model will have to be checked experimentally.
- 7.3 Experimental and analytical investigations should be conducted to establish how flushing fluid flows past the buttons on the face of bits. This will help refine the computer model.
- 7.4 The amount of chip regrinding which occurs during rotary percussion drilling has never been determined. This may be due to the extreme difficulty of obtaining an accurate and reliable measure of the size of chips as they are formed. If a technique could be developed, regrinding could be quantified. It would also provide a measure of the efficiency of different bit designs and drilling systems.
- 7.5 It appears as if relationships exist between chip sizes, drilling parameters, drilling equipment design and rock properties (see section 5.1.2). If the nature of these relationships could be determined it will contribute greatly to a better understanding of the drilling process.

- 7.6 The computer model assumes that the rock at the end of the hole is smooth and that the buttons make point contact with it. If the profile of the end of percussion drilled holes could be measured it will eliminate the need to make assumptions about it. The distance between the end of the hole and the face of the bit is crucial to the accuracy of modelling flushing. Measurement of the profile of the end of hole may also reveal a great deal about the mechanism of rock breaking.

## APPENDIX A

## EQUIPMENT AND APPARATUS

## A 1 FOR DRILLING WITH 48 mm DIAMETER BITS

## A 1.1 ROCKDRILL

Long stroke version of Boart Longyear HD-150 hydraulic drill. According to the manufacturers, performance at 17 MPa percussion pressure is:

Blow energy                   = 225 J  
Percussion power           = 11.4 kW

## A 1.2 DRILL RIG

Fully hydraulic single boom jumbo, sold by Boart Longyear under the name "Benchmaster". Percussion, rotation and feed pressures all manually controlled.

## A 1.3 DRILLING CONSUMABLES

Bits - 48 mm nominal diameter with six 11 mm diameter gauge buttons and two 8 mm diameter face buttons. One face and 2 flute flushing holes, all 6 mm diameter. All buttons hemispherical.

Rods - 32 mm across flats hexagonal and 3.1 m nominal length. Flushing hole diameter = 8.5 mm. Male threaded both ends.

All current (1997) standard Boart Longyear products for the South African market.

#### A 1.4 MISCELLANEOUS

Diesel engine driven, 2 stage centrifugal water pump, model 2/25-200 from local supplier, Pumpco.

#### A 2 FOR MEASURING ROCKDRILL FREQUENCY

Oscilloscope - Digital storage type. Explorer 1, model 2090-I, manufactured by Nicolet Instrument Corp. of the USA.

Pressure transducer - 25 MPa capacity with 4 to 20 mA output, model 2000B, from Transinstrument of the UK.

A resistor (approximately 150  $\Omega$ ) placed across the pressure transducer output terminals provided a voltage signal for the oscilloscope.

#### A3 FOR DRILLING WITH 36 mm DIAMETER BITS

Boart Longyear pneumatic rockdrill, model S-23. Rated performance at applicable supply air pressure of 430 kPa as follows:

Percussion frequency	= 28.5 Hz
Blow energy	= approximately 61 J, therefore
	percussion power is approximately 1.74 kW
Rotational speed	= 124 rpm

It was attached to a rig built specifically for experimental drilling. The rig includes an air cylinder (parallel to the rockdrill) which provides thrust or feed force.

Bits - 36 mm nominal diameter with three gauge and one face buttons, all 9 mm diameter, with conical shape. Attached to the drill rod with a 11° self locking taper.

Rods - 22 mm across flats hexagonal, 1.8 m long and fitted with rubber collar. Flushing hole approximately 6 mm diameter.

A 4 FOR ANALYSING CHIP SAMPLES

Sieves with the following mesh sizes:

2.0, 1.4, 1.18, 0.6, 0.355, 0.25 and 0.075 mm.

Libror AEU-130 chemical balance, supplied by Shimadzu.



## APPENDIX B

## COMPUTER MODEL

A listing, sample input and output are at the end of the Appendix while a flow chart is given in figure 4.1. The flow chart and listing are for the 48 mm diameter bits, because these items do not differ significantly from those for the 36 mm diameter bits.

The programme was written using the Windows version of TK Solver. It does not recognise the Greek alphabet, subscripts and superscripts, therefore:

- The symbols for many variables consist of more than one letter on the same line. For example chip velocity is vc.
- The symbol ^ indicates raising to a power. For example fluid velocity squared is vf^2.
- Where a letter from the Greek alphabet would normally be used to indicate particular quantities, the name of the Greek letter is used instead. For example "rho" instead of  $\rho$  for density.

Constructions such as 'vfr,i and 'vfr[i] indicate a particular value of the variable vfr (radial component of fluid velocity) where i is simply a counter. Place('t,i) means put the current value of t in position i in the list t. A word followed by a colon names and marks the beginning of a new part of the programme. An asterisk indicates multiplication.

TK Solver always starts with a "rule sheet", but looping and iteration can only be done in "procedures". Thus the listing is split into a rule sheet and a procedure named "flush". The rule sheet is very short and simple, therefore it is not included in the flow chart. Only the procedure (flush) is in the flow chart.

Measurement units which are commonly accepted in the drilling industry are used for the sample input and output quantities in section B11. Thus bit and hole dimensions are in mm, rockdrill frequency is in blows per minute (bpm), bit rotational speed is in rpm, penetration rate is in cm/min and flow rates are in l/min. However a separate routine was included to convert all these to SI units - which were used for all the calculations. Thus the equations on the rule sheet and procedure function listing do not usually include conversion factors.

## B1 MODELLING PROCEDURE

The model simulates movement of a chip from its formation on the end of the hole until it enters the annulus between the outside of the bit and the side of the hole. As shown in the flow chart (see figure 4.1) it uses nested loops and iteration. The main output from each model run is a prediction of the minimum flow rate required to flush a chip of a defined size and shape from a given radial position to the annulus.

Starting from an initial low flow the outer loop increases the flow rate until the chip reaches the annulus in the time between hammer blows.

Each cycle through the inner loop calculates how far the chip moves in a single short time step. Water velocity, chip velocity and acceleration are held constant for the duration of each step. Thus the inner loop uses chip position and the previous values of water velocity and chip velocity, to update chip position. This in turn is an input to the calculation of water velocity, which is combined with chip velocity for calculating chip acceleration. Chip velocity and displacement are calculated from chip acceleration and the duration of the step.

At the end of each step the model compares the updated value of chip displacement with the distance from the chip's starting point to the annulus. If the chip has not yet reached the annulus it compares elapsed time since chip movement started with the time between hammer blows. If either elapsed time or chip displacement are too big the outer loop increases the flow rate and the process is repeated.

Most calculations are in the inner loop. The main steps were calculation of:

- Water velocity at the chip;
- Force due to drag on the chip;
- Chip acceleration and resulting position at the end of the time step;
- Elapsed time.

If the elapsed time was greater than the time between percussive impacts then flow rate was increased and the calculations repeated. If not, the procedure was repeated until the chip either reached the annulus or the elapsed time became too great.

The model was for a single chip. However the effect of other chips in reducing the cross sectional area available for fluid flow was taken into account.

## B2 CO-ORDINATE SYSTEM

The model predicts flow rates for a rotating bit. Thus, there was no need to take the orientation of the bit into account. The co-ordinate system was developed to suit chip movement, which is predominately, but not exclusively radial. The features of the co-ordinate system were:

- A radial line from the centre of the bit (and hole) to the wall of the hole provided the basic reference.

- This reference line was kinked to follow the profile of the end of a button bit (see figure B1).
- Points were located by distance along a radius and distance perpendicular to the radius (see figure B2).
- The origin of the co-ordinate system was at the centre of the bit.

Thus the co-ordinates for chip position were:

sr = radial distance (following the profile of the bit) from the centre line of the bit and hole to the centre of chip

sa = distance perpendicular to the radius along which sr was measured

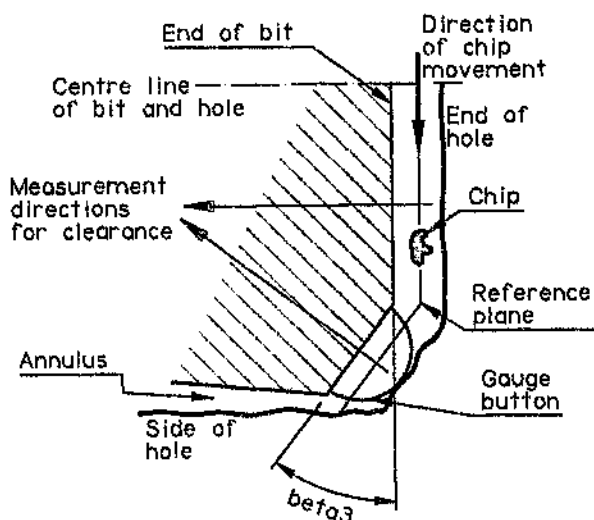


Figure B1 Kinked reference plane

Since the analysis was essentially two dimensional a third co-ordinate was not necessary. Clearance between the bit and the end of the hole was measured perpendicular to the face of the bit at the relevant radius.

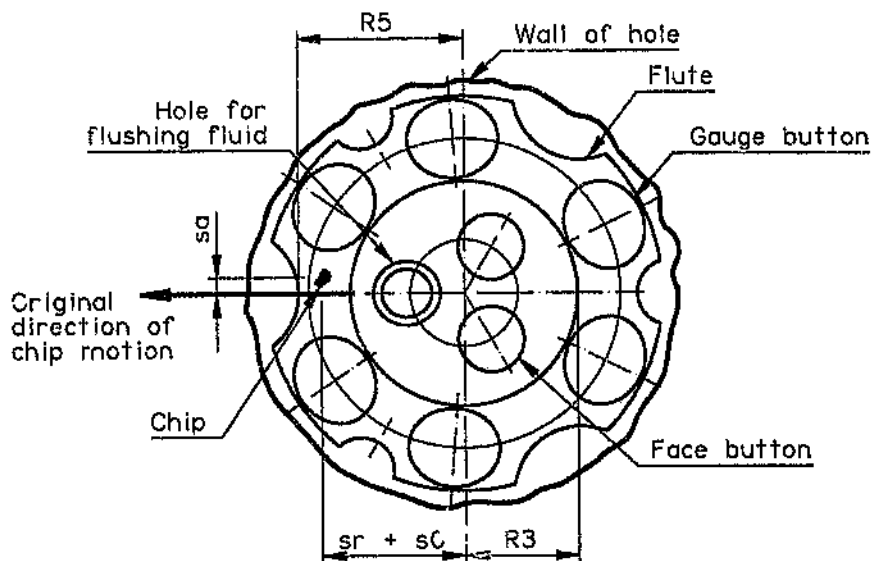


Figure B2 Co-ordinate system

### B3 DISTANCE WHICH THE CHIPS HAD TO MOVE

This distance ( $sr_{max}$ ) was a function of:

- The radial co-ordinate of the position at which the chip was formed.
- The average radius to the flutes on the bit, or in other words, the average distance to the annulus between the bit and the wall of the hole.
- The profile of the end of the bit.

Thus,

$$sr_{max} = R3 + (R5 - R3)\cos(\beta3) - s0$$

where

- $R3$  = radius of the central part of the end of the bit which is perpendicular to the axis of the bit (see figure B2)
- $R5$  = average radius to the start of the flutes (see figure B2)
- $\beta3$  = the angle of the outer part of the bit (see figure B1)

$s_0$  = initial position of the chip = distance  
from the axis of the bit to the centre of  
the chip

#### B4 CROSS SECTIONAL AREA FOR FLOW

##### B4.1 FLOW AREA

At any flow rate the radial component of fluid velocity depends on the cross sectional area available for flow. For radially outward flow, cross sectional area = circumference x effective clearance between the bit and the end of the hole.

$$\text{Circumference} = 2.\pi.s_r$$

where  $\pi$  = ratio of the circumference of a circle to its diameter = 3.1416...

$s_r$  = radial distance (following the profile of the bit)

Effective clearance was a function of the shape, size and position of the buttons on the bit, as well as the location of the flushing holes.

##### B4.2 ALLOWANCE FOR BUTTON SHAPE

The buttons result in the cross sectional area available for flushing flow varying in a complex and irregular way in all three dimensions. Exact equations specifying cross sectional area could have been developed, but each bit design would need its own set of equations. Since the equations would be very involved, this option would dramatically reduce the accessibility of the computer model. Therefore a method of approximating clearance was developed. To allow modelling of flushing to be available to as wide a range of people as possible it seemed appropriate that the method of approximating clearance should:

- Be understandable enough to be applied by drawing office personnel as a routine procedure during button bit design;
- Not need too many additional input variables because of the limitations of TK Solver.

Hemispherical buttons (as on the 48 mm diameter bits used in the drilling experiments) were approximated by cylinders with diameter =  $0.85 \times$  nominal button diameter. The factor (0.85) was based on figure B3. When taking a section through the length of the button the area (B) added on the "rock side" is somewhat greater than the area (A) lost near the face of the bit. Hence, 0.85 includes an allowance for button wear.

Following a similar reasoning, conical buttons (such as on the 36 mm diameter bits) were replaced by cylinders with diameter =  $0.7 \times$  nominal button diameter (see figure B4).

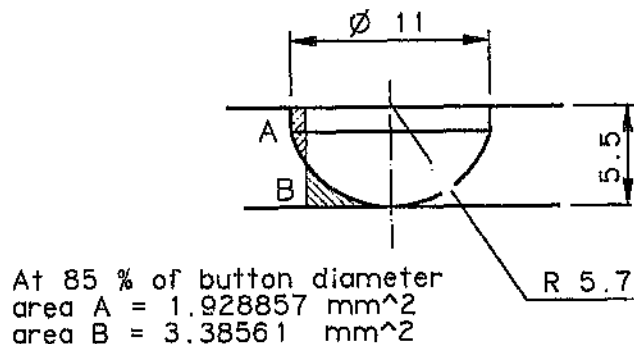


Figure B3 Approximation to hemispherical button shape

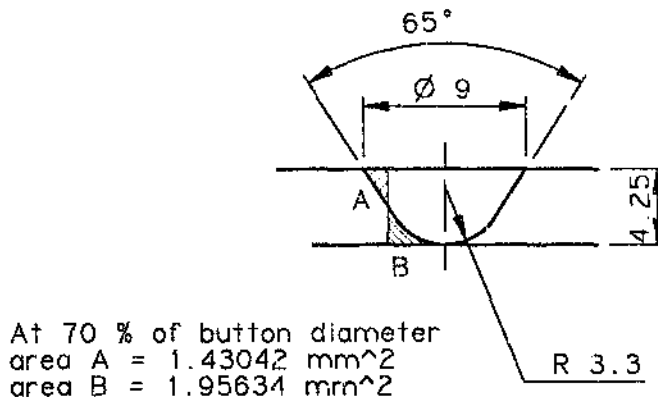


Figure B4 Approximation to conical button shape.

#### B4.3 ALLOWANCE FOR BUTTON SIZE AND POSITION

The face of the bit was then divided into five annular sections. As shown in figure B5, they were chosen such that:

- The outside diameter of the outer section was equal to the average flute diameter of the bit.
- The diameter of the flat part of the face of the bit was a dividing line.
- The sections were approximately uniformly spaced.

Effective clearance for each of the annular sections was then determined by:

- Making a plan view of the face of the bit with the buttons replaced by circles with diameter = 0.85 or 0.7 times button diameter.
- Calculating effective clearances  $x_1$ ,  $x_2$ ,  $x_3$ ,  $x_4$  and  $x_5$  using the equation:  

$$\text{effective clearance} = (\text{total area} - \text{sum of areas not available for flow}) / \text{total area}.$$

Where area not available for flow = area occupied by buttons + area of face flushing holes
- Multiplying effective clearance by the resultant button protrusion.



- $x_1 = 0.771$ )excluding area of face  
 $x_2 = 0.536$ )flushing hole and its chamfer  
 $x_3 = 0.958$   
 $x_4 = 0.516$ )taking flow pattern  
 $x_5 = 0.399$ )into account

"X" indicates: flushing hole

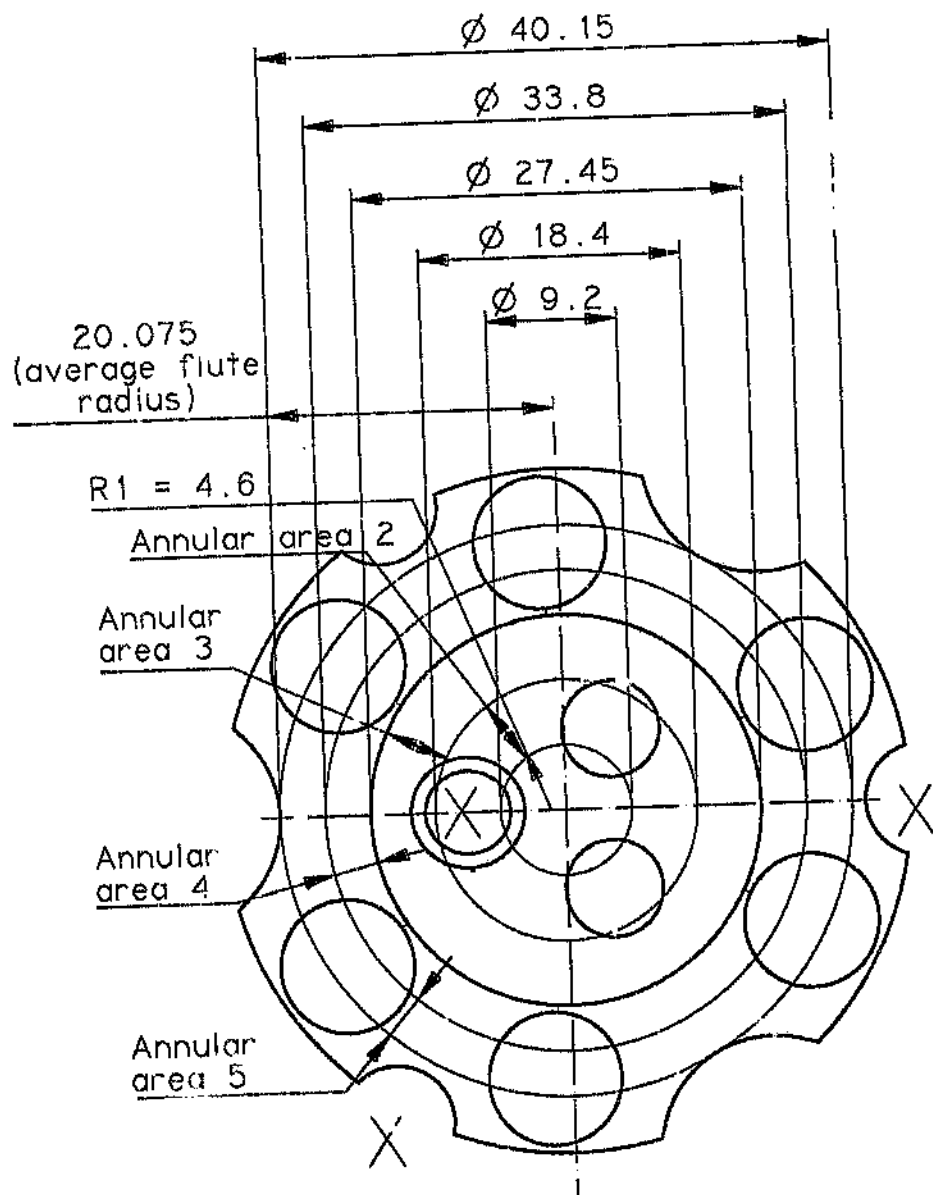


Figure B5 Clearances for the 48 mm diameter bit

#### B4.4 ALLOWANCE FOR NON-RADIAL FLUSHING FLOW

Since they were standard items, both bits used had:

- A face flushing holes offset from the centre-line of the bit.
- Flushing holes in one or more flutes.

The model assumed that the flow was purely radial and outwards. However due to the placement of the flushing holes, the actual flows did not conform to the radial flow assumption. Nevertheless, the flow was still sufficiently radial for the model to be useful. The clearances were modified where necessary to account for non-radial flow.

The division of flow between the various flushing holes was determined experimentally. Thereafter the flow patterns shown in figures B6 and B7 were derived according to the following reasoning:

- Water flows radially outwards from face flushing holes and the flow is uniformly distributed around the circumference of the hole. Thus, for example, the flow labelled "2" in figure B6 is  $117.3/360$  of the flow from the face flushing hole.
- Water leaving a flushing hole in a flute flows radially inward until it reaches the face of the bit. Thereafter it curves around the nearest gauge buttons to exit from the closest flutes without flushing holes.

The resulting flow patterns are shown in figures B6 and B7.

"X" indicates flushing hole.  
Width of arrows indicates  
relative volume flow rates.

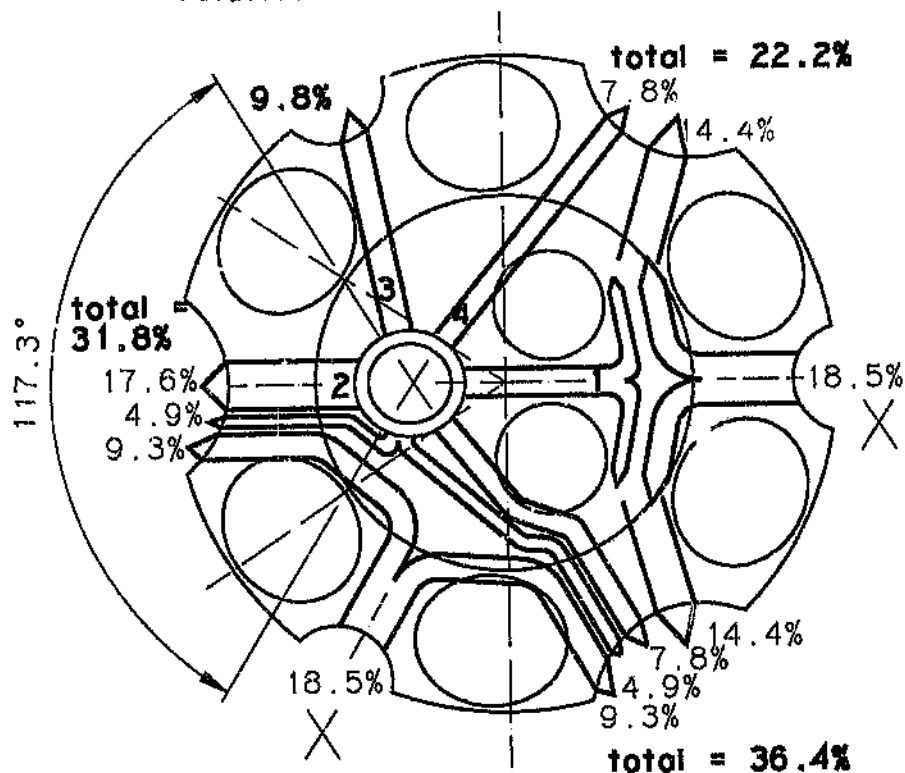


Figure B6 Probable flow pattern for the 48 mm diameter bit

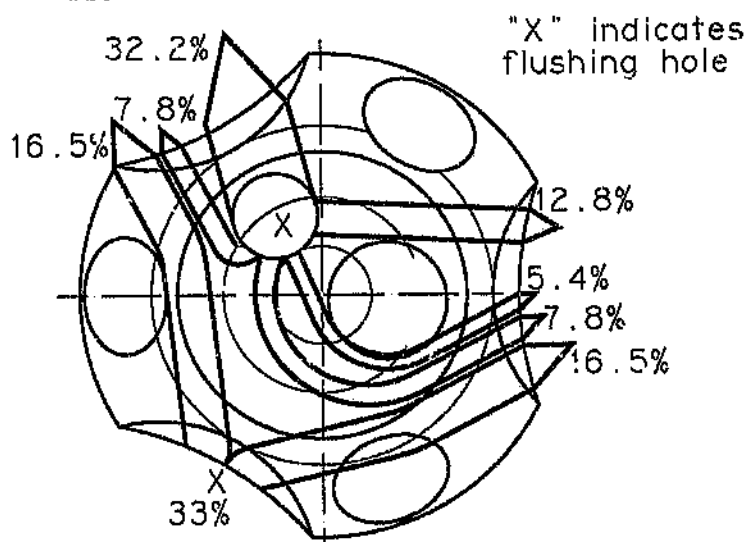


Figure B7 Probable flow pattern for the 36 mm diameter bit

## B5 PENETRATION RATE

The cross sectional area available for fluid flow was reduced by chips in the gap between the bit and the end of the hole. However, the actual concentration of chips in the flushing fluid was unknown. For the purposes of developing an allowance for penetration rate, the following approximations were made:

- Irrespective of where they were formed on the end of the hole, all chips were only just removed in the time between hammer blows.
- Chip concentration in the fluid was uniform.

Since chip production rate (by volume) = penetration rate x hole diameter, the correction (y) was applied:

$$y = 1 - (5p / (f(cx1 + cx2 + cx3 + cx4 + cx5)))$$

where      y = 1 - blockage due to the chips  
             p = penetration rate  
             f = hammer frequency  
             cx1 to cx5 = effective gap between the end of the bit and the end of the hole (taking buttons into account)

For 48 mm diameter bits the chips reduced the cross sectional area available for flow by about 15 % (see "y" in figure B9. Thus even if the correction was not quite right, the error would have been small.

## B6 FLUID FLOW

Combining some of the factors already discussed with continuity gave the following relation for the radial component of fluid velocity.

$$v_{fr} = Q / 2\pi \cdot sr \cdot cx \cdot y$$

where       $v_{fr}$  = radial component of fluid velocity

Q = volume flow rate  
 cx = effective clearance

Due to bit rotation the circumferential velocity of the fluid adjacent to the bit had to equal the bit's circumferential velocity. The end of the hole is stationary so the circumferential velocity of the fluid adjacent to it had to be zero. Thus the average circumferential velocity of the fluid was taken as the average of these ie. - half the circumferential velocity of the bit at a radius corresponding to the chip position. Or in symbols:

$$v_{fa} = \pi \cdot N \cdot sr / 60$$

where N = bit rotational speed in rpm

The resultant flow velocity was then

$$v_f = \sqrt{(v_{fr}^2 + v_{fa}^2)}$$

## B7 CHIP ACCELERATION

The most important forces on the chip are drag, weight and buoyancy. Drag acts in the same direction as fluid flow. The holes were horizontal and fluid flow in the gap between the end of the bit and the end of the hole was approximately radial. Therefore, the fluid and chips moved more or less in a vertical plane but at various orientations within the plane (see figures B1 and B2).

The weight and buoyancy vectors act in the plane of fluid and chip motion. However, since fluid flow and chip motion occurred in all possible orientations within the vertical plane, the effects of weight and buoyancy could be disregarded. In other words, on average as many chips were moving radially upwards against gravity as were moving radially downwards with assistance from gravity. Thus, acceleration (a) was calculated from the commonly accepted equation for drag on a submerged body in subsonic flow [Douglas, Gasiorek and Swaffield<sup>[16]</sup>].

$$a = \frac{C_d \cdot \rho \cdot A (v_f - v_c)^2}{2m}$$

where  $C_d$  = drag coefficient  
 $\rho$  = density of fluid (water)  
 $A$  = maximum cross sectional area of the chip  
 $m$  = mass of the chip

Drag was total or profile drag. The appropriate coefficient, taking both pressure drag and skin friction into account was used.

Maximum cross sectional area was used because Bain and Bonnington<sup>(13)</sup>, Zandi and Govatos<sup>(14)</sup> and Graf<sup>(15)</sup> all state that broadside on orientation is most common, especially at Reynold's numbers in the Newton Flow range.

From measurements of settling velocity, McFadzean<sup>(5)</sup> estimated the drag coefficient of chips in the Newton flow regime to be three times the drag coefficient for a sphere (ie. - 3 x 0.44). Beddow, Fong and Vetter<sup>(20)</sup> also found that irregularly shaped particles have much higher drag coefficients than spheres. Since McFadzean's chips were produced by rotary percussion drilling into the same type of rock (Witwatersrand quartzite), there was no need to re-estimate the drag coefficient.

Slip velocity (the difference between fluid and chip velocity or  $v_f - v_c$ ) varied over a wide range. Thus the programme includes equations from Dougherty and Franzini<sup>(19)</sup> for drag coefficient in the Stokes and Allen flow regimes as well.

Reynold's number ( $Re$ ) was used to determine which flow regime was applicable. For calculating Reynold's number, chip equivalent diameter ( $d_{eq}$ ) provided the length term and slip velocity provided the velocity term. Chip equivalent diameter was defined as the diameter of a sphere with the same volume as the chip.

## B8 CHIP VELOCITY, DISPLACEMENT AND ELAPSED TIME

Acceleration was assumed constant for each short time interval. Therefore the well known equations for constant acceleration straight line motion [Gieck<sup>(21)</sup>] were used to calculate both components of chip velocity and displacement. The resultants are calculated from the components.

Incremental displacements were used to calculate new coordinates for the position of the chip at the end of each time step. The durations of each time step were added to give the elapsed time since the chip was formed.

Initially when the chip is stationary with fluid moving past it, the drag coefficient for Newton flow applies. Then as the chip accelerates and moves towards the annulus, the slip velocity decreases so that first the Allen and then Stokes flow regimes become applicable. In the Stokes' flow region drag coefficient was taken as  $C_d = 3 \times 24/Re$ , for  $Re = \rho(v_f - v_c)ced/\mu$

where  $Re$  = Reynold's number  
 $\rho$  = density of fluid  
 $v_f$  = fluid velocity  
 $v_c$  = chip velocity  
 $ced$  = chip equivalent diameter = diameter of a sphere with the same volume as the chip  
 $\mu$  = dynamic viscosity of fluid

Combining these two equations gives

$$C_d = 72.\mu/\rho(v_f - v_c)ced$$

Thus as chip velocity tends towards fluid velocity, drag coefficient increases rapidly. In the absence of other retarding forces, this will result in the chips moving at exactly the same speed as the fluid. However the chips do not move in isolation. In the model chip velocity was limited to 0.95 times fluid velocity because:

- Chip/chip, chip/hole and chip/bit interactions (collisions) will slow the chips down.
- The model became unstable when slip velocity ( $v_f - v_c$ ) was close to zero.

#### B9 ENDING

Once the chip had travelled far enough to enter the annulus, the elapsed time was compared to the time between hammer blows. If the elapsed time was less then the chip had been flushed out quickly enough and the flow rate was outputted. If not, the flow rate was incremented and all the calculations were repeated for the higher flow rate.

#### B10 INPUT CONSTANTS

The starting flow rate, time and flow rate increments are set in terms of other variables at the beginning. The size of the increments were determined by trial and error to give reasonable results without excessively long run times.

Since fluid temperature was close to 20° C dynamic viscosity of water was taken as 0.001 kg/ms and density was taken as 998 kg/m<sup>3</sup> [Daugherty and Franzini<sup>(19)</sup>].

#### B11 PROGRAMME LISTING, INPUT AND OUTPUT

##### S Rule

;LISTING OF MODEL FOR 48 mm DIAMETER BUTTON BITS, WITH WATER FLUSHING;

```
* cx1=c1*x1
* cx2=c2*x2
* cx3=c3*x3
* cx4=c4*x4
* cx5=c5*x5

* call flush(cx1,cx2,cx3,cx4,cx5,A,V,f,s0,m,p,R1,R2,R3,R4,R5,beto3,N1,vf,a,vc,s,QB,y,it,Q1,gr,ss,vcr,vc
```

;COMMENT: "call flush" is the command for switching to the procedure function "flush" (see overleaf).



Comment:	Procedure for 48 mm diameter bit
Parameter Variables:	
Input Variables:	cx1,cx2,cx3,cx4,cx5,A,V,f,s0,m,p,R1,R2,R3,R4,R5,beta3,N
Output Variables:	t,vf,a,vc,s,QB,y,it,Q1,sr,sa,vcr,vca,srmax,Res0,Re,vfs0
<u>S</u> <u>Statement</u>	

```

y=1-(5*p/(f*(cx1+cx2+cx3+cx4+cx5)))
lt=1/(100*f)
srmax=(R3+((R5-R3)/(cos(beta3))))-s0
Q1=(srmax^2)/2
IQ=Q1/10
Q=Q1
ced=(6*V/PiQ)^0.33333

```

```

initiate:
i=1
t=0
sr=s0
sa=0
vcr=0
vca=0
vc=0

beta=0
if sr>=R3 then beta=beta3

```

```

cx=cx1
if sr>=R1 then cx=cx2
if sr>=R2 then cx=cx3
if sr>=R3 then cx=cx4
if sr>=R4 then cx=cx5

```

```

call listcopy('zero','t')
call listcopy('zero','vf')
call listcopy('zero','a')
call listcopy('zero','vc')
call listcopy('zero','s')

```

```

start:
if i=1 then lt=i/10
if i=2 then lt=lt*5
if i=3 then lt=lt*2
t:=t+lt
PLACE('t,i)=t
if t>=0.97/f then Q:=Q+IQ else goto resume
goto initiate

```

S Statement

resume:

place('vfr,i)=Q/(2\*Pi()\*sr\*cx\*y)

place('vfa,i)=Pi()\*N\*sr/60

place('vf,i)=(vfr[i]^2+vfa[i]^2)^0.5

vfr='vfr[i]

vfa=('vfa[i]

vf=('vf[i]

Re=998\*(abs(vf-vc))\*ced/0.001

Cd=3\*18.5/(Re^0.6)

if Re&lt;0.2 then Cd=3\*24/Re

if Re&gt;500 then Cd=3\*0.44

ar=(Cd\*998\*A\*('vfr[i]-vcr)\*abs('vfr[i]-vcr))/(2\*m)

aa=(Cd\*998\*A\*('vfa[i]-vca)\*abs('vfa[i]-vca))/(2\*m)

a=(ar^2+aa^2)^0.5

PLACE('ar,i)=ar

PLACE('aa,i)=aa

loop.

vcr=vcr+ar\*it

vca=vca+aa\*it

vc=(vcr^2+vca^2)^0.5

if vc&gt;=0.95\*vf then goto steady

PLACE('vcr,i)=vcr

PLACE('vca,i)=vca

PLACE('vc,i)=vc

goto continue

steady:

vcr=0.95\*vfr

vca=0.95\*vfa

vc=(vcr^2+vca^2)^0.5

PLACE('vcr,i)=vcr

PLACE('vca,i)=vca

PLACE('vc,i)=vc

continue:

sr=sr+vcr\*it+0.5\*ar\*it^2

sa=sa+vca\*it+0.5\*aa\*it^2

s=(sr^2+sa^2)^0.5

PLACE('sr,i)=sr

PLACE('sa,i)=sa

PLACE('s,i)=s

S Statement

```

beta=0
if sr>=R3 then beta=beta3

cx=cx1
if sr>=R1 then cx=cx2
if sr>=R2 then cx=cx3
if sr>=R3 then cx=cx4
if sr>=R4 then cx=cx5

i:=i+1
if sr>=srmax+s0 then goto time else goto start

time:
if t>=0.97/f then Q:=Q+iQ else goto end
goto Initiate

end:
QB=Q
vf=vf[i-1]
vfo=vf[1]
t=t[i-1]

Res0=998*vf[1]*ced/0.001
Re=998*vf*ced/0.001

```

Figure B8 Programme listing

<u>St</u>	<u>Input</u>	<u>Name</u>	<u>Output</u>	<u>Unit</u>	<u>Comment</u>
MODEL FOR 48 mm DIAMETER BITS					
2940 bpm, 197 rpm, 120 cm/min very large flat chip starting at 8 mm					
	4.6	R1		mm	outside radius of centre of flat face
	9.2	R2		mm	
	13.725	R3		mm	outside radius of flat on face of bit
	16.9	R4		mm	
	20.075	R5		mm	average radius at start of flutes
	30	beta3		deg	angle of gauge button surface
	4	c1		mm	
	4	c2		mm	clearance between bit and hole bottom
	4	c3		mm	
	5.5	c4		mm	
	5.5	c5		mm	
	.771	x1			
	.636	x2			1 - blockage due to buttons
	.858	x3			
	.516	x4			
	.389	x5			
		cx1	3.084	mm	
		cx2	2.144	mm	effective clearance
		cx3	3.832	mm	
		cx4	2.838	mm	
		cx5	2.1945	mm	
	39	A		mm^2	chip cross sectional area
	.2	m		g	chip mass
	76	V		mm^3	chip volume
	2940	f		bpm	hammer frequency
	197	N		rpm	bit rotation speed
	120	p		cm/min	penetration rate
	8	s0		mm	initial position of chip
		smax	13.057348	mm	radial distance to flute from s0
L	998	rho		kg/m^3	density of flushing water
	.001	vis		kg/ms	dynamic viscosity
		it	.00020408	s	time increment
		y	.85518422		blockage under bit due to chips
I		s	21.058593	mm	total distance between chip and bit
		sr	21.057649	mm	axis when chip enters annulus
		sa	.1993224	mm	radial distance
					circular displacement

<u>St</u>	<u>Input</u>	<u>Name</u>	<u>Output</u>	<u>Unit</u>	<u>Comment</u>
L		t	.01971429	s	time since chip started moving
L		vc	.67904074	m/s	chip velocity at entry into annulus
		vcr	.87869547	m/s	radial component of chip velocity at annulus
		vca	.01404502	m/s	angular component of chip velocity at annulus
		vfs0	2.0349431	m/s	fluid velocity at s0
		vf	.76063597	m/s	fluid velocity at smax
L		a	.94698107	m/s^2	chip acceleration at entry into annulus
		Q1	5.1148304	l/min	starting flow rate under bit
		ced		mm	equivalent diameter of chip
		Res0	10873.692		Reynold's no. of chip at s0
		Re	3989.662		Reynold's no. of chip at flutes
		QB	11.252627	l/min	fluid volume flow rate for optimal flushing of large flat chip starting at s0

Figure B9 Samp'e input and output

## APPENDIX C

## SUPPORTING CALCULATIONS

## C1 EFFECT OF ROTATION ON FLOW PATHS

Flow visualization suggested that at low flow rates there is a free water surface between the face of the bit and the end of the hole. The possible position of a free surface was investigated by observing the flow from stationary bits at different orientations and flow rates. However, the technique's validity is dependant on the circumferential component of fluid velocity (caused by bit rotation) being much smaller than the axial component.

If the origin of co-ordinates is in the centre of the face of the bit the components of flow velocity are:

- Axially perpendicular to and away from the face of the bit.
- Circumferential or perpendicular to a radial line on the face of the bit.

Consider a 48 mm diameter bit because these are larger and their rotational speed was higher than that for the 36 mm diameter bits. The cross sectional area (A) of the face flushing hole is:

$$A = \pi.D^2/4$$

where  $\pi$  = ratio of circumference to diameter of a circle = 3.1416...  
 $D$  = hole diameter = 6 mm

so

$$\begin{aligned} A &= \pi \times 0.06^2/4 \\ &= 2.827 \times 10^{-5} \text{ m}^2 \end{aligned}$$

Assume the flushing flow rate ( $Q$ ) is 5 l/min, because flow visualization suggested that this should give slightly less than complete coverage of the face of the bit (see section 5.2.2). It is also the flow at which penetration rate first becomes constant and independent of flushing. Measurement of the flow from each flushing hole showed that 63 % left from the face hole. Therefore, in  $\text{m}^3/\text{s}$ , the flow ( $q$ ) from the face hole only was:

$$\begin{aligned} q &= 0.63 \times 5/60 \times 1000 \\ &= 5.25 \times 10^{-5} \text{ m}^3/\text{s} \end{aligned}$$

Thus, axial or jet velocity ( $v_j$ ) of the flow from the face flushing hole is:

$$\begin{aligned} v_j &= q/A \\ &= 5.25 \times 10^{-5} / 2.827 \times 10^{-5} \\ &= 1.86 \text{ m/s} \end{aligned}$$

The circumferential velocity ( $v_c$ ) imparted to the flow by the rotation of the bit is:

$$v_c = \omega \cdot r$$

where  $\omega$  = angular velocity of bit  
 $r$  = distance from the axis of the bit to the  
 centre of the face flushing hole = 6.9 mm

Bit rotational speed ( $N$ ) was 197 rpm, therefore

$$\begin{aligned} \omega &= 2\pi N/60 \\ &= 2\pi \cdot 197/60 \\ &= 20.63 \text{ rad/s} \end{aligned}$$

so

$$\begin{aligned} v_c &= 20.63 \times 0.0069 \\ &= 0.142 \text{ m/s} \end{aligned}$$

Thus axial velocity is  $1.86/0.142 = 13.1$  times greater than angular velocity. Hence bit rotation is unlikely to have a significant effect on flow.

## C2 ENERGY REQUIRED TO CREATE UNIT AREA OF NEW SURFACE

Equation 12 from section 5.1.2 can be written as

$$k = \frac{4 \cdot r \cdot (dE/dt)}{3 \cdot \pi \cdot D^2 \cdot (dl/dt)}$$

where  $r$  = radius of a spherical chip with volume equal to that of a typical non-spherical chip

$dE/dt$  = percussion power input to hole

$\pi$  = ratio of circumference of a circle to its diameter = 3.1416 ...

$D$  = diameter of hole drilled by button bit

$dl/dt$  = penetration rate

Unfortunately the size fractions into which the chip samples were split are too large for an accurate determination of the size of a typical chip. Therefore, for the purposes of this calculation assume that the volume of a typical chip is the mean of the volumes of the extreme sized chips (see section 5.1.1) - in other words the average of the volumes of a minute cubic chip and a very large flat chip. However the volume of the minute cubic chips is more than five orders of magnitude less than the volume of the chips at the other end of the size range. Thus the average volume can be taken as half the volume of the very large flat chips. So from equation 1 in section 5.1.2

$$r = ((3 \cdot V_i)/(4 \cdot \pi))^{0.333}$$

where  $V_i$  = volume of a typical chip



Further assumptions are:

- Maximum penetration rate
- Hole diameter 2 mm greater than bit diameter because small button bits are typically drill holes slightly greater than the diameter of the bit.

Hence for the 48 mm diameter bit and hydraulic rockdrill

$$V_b = 76/2 = 38 \text{ mm}^3$$

$$dE/dt = 11.4 \text{ kW (see Appendix A)}$$

$$D = 48 + 2 = 50 \text{ mm}$$

$$dl/dt = 103 \text{ cm/min. (see figure 5.5)}$$

$$= 1.03/60 = 0.0172 \text{ m/s}$$

so

$$r = (3 \times 38 \times 10^{-9} / 4 \times \pi)^{0.333}$$

$$= 2.09 \times 10^{-3} \text{ m}$$

and

$$k = \frac{4 \times 2.09 \times 10^{-3} \times 11.4 \times 10^3}{3 \times \pi \times 0.05^2 \times 0.0172}$$

$$= 2.35 \times 10^5 \text{ W/m}^2$$

$$= 0.235 \text{ W/mm}^2$$

Similarly for the 36 mm diameter bit and pneumatic rockdrill

$$V_b = 38/2 = 19 \text{ mm}^3$$

$$dE/dt = 1.74 \text{ kW (see Appendix A)}$$

$$D = 36 + 2 = 38 \text{ mm}$$

$$dl/dt = 65 \text{ cm/min (see figure 5.5)}$$

$$= 0.65/60 = 0.0108 \text{ m/s}$$

so

$$r = (3 \times 19 \times 10^{-9} / 4 \times \pi)^{0.333}$$

$$= 1.67 \times 10^{-3} \text{ m}$$

and

$$k = \frac{4 \times 1.67 \times 10^{-3} \times 1.74 \times 10^3}{3 \times \pi \times 0.038^2 \times 0.0108}$$

$$= 7.9 \times 10^4 \text{ w/m}^2$$

$$= 0.079 \text{ w/mm}^2$$

### C3 CHIP ACCELERATION UNDER GRAVITY ALONE

A newly loosened chip at rest on the unflushed part of the end of the hole is subject to a constant acceleration due to gravity. Neglecting all retarding forces (such as air resistance and mechanical friction), the maximum distance which such a chip can move in the time between hammer blows is given by the well known equation for straight line constant acceleration motion [Gieck<sup>(21)</sup>]:

$$s = u.t + 0.5a.t^2$$

where       $s$  = displacement in m  
               $u$  = initial velocity = 0  
               $t$  = elapsed time = typical time between hammer  
                                  blows for a hydraulic drill = 0.0198 s  
               $a$  = acceleration = gravitational acceleration =  
                                  9.81 m/s<sup>2</sup>

so

$$s = 0 + 0.5(9.81 \times 0.0198^2)$$

$$= 0.0038 \text{ m} = 3.8 \text{ mm}$$

Since the distance from top to bottom of the unflushed part of the hole may be 20 mm or more many chips will not be removed from the unflushed part of the end of the hole in the time between hammer blows.

$$F = (\pi \times 0.075^2 \times 250\,000) = 552 \text{ N}$$

## APPENDIX D

## DETAILED DATA

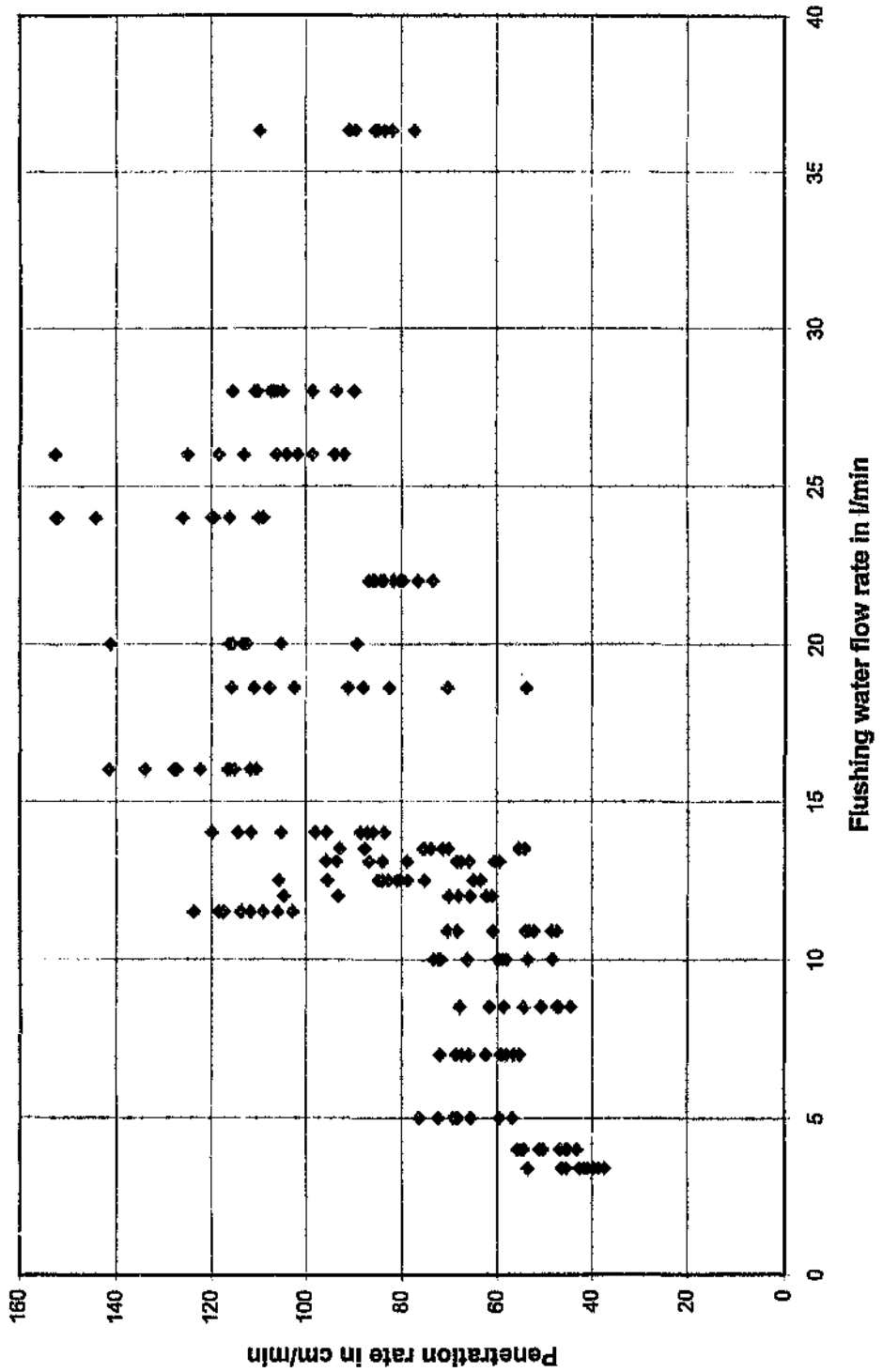
## D1 DRILLING DATA

Table D1 Drilling data for 36 mm diameter bits

Flow rate (l/min)	Penetration rate (cm/min)
0.72	34.2
1.0	41.9
1.0	46.1
1.0	45.0
1.3	57.9
1.3	57.0
1.7	65.0
2.8	70.7
3.8	62.0
3.5	69.9
5.0	61.7
5.6	63.9
8.8	62.9
10.0	64.1
15.9	48.1
15.9	66.7
16.3	70.0
20.0	64.3
20.0	64.8
20.9	72.0

Table D2 Summary of drilling data for 48 mm diameter bits

Flow rate (l/min.)	Average penetration rate (cm/min.)	Standard deviation
3.4	42.6	4.76
4.0	49.2	4.68
5.0	68.4	5.97
7.0	62.5	5.67
8.5	53.8	7.24
10.0	62.2	8.38
10.9	56.1	7.84
11.5	113.4	6.64
12.0	81.8	16.96
12.5	74.9	12.16
13.1	76.0	13.44
13.5	69.1	12.74
14.0	105.2	13.11
16.0	122.2	13.15
18.6	91.4	20.34
20.0	113.8	12.70
22.0	81.8	4.35
24.0	125.9	17.46
26.0	110.5	18.15
28.0	104.4	8.04
36.3	88.0	8.75



## D2

## RESULTS OF MODEL RUNS

The meanings of the headings in the next two tables are:

Initial position: Radial position of chip when it is formed, ie. - its initial radial position.

Minimum flow rate: Flow required to move the chip from its initial radial position to the annulus in the time between hammer blows.

Minute cubic chip: One which is shaped like a cube with length of side equal to 0.05 mm.

Average large flat chip: One with shape and dimensions based on those for a typical chip in the largest size fraction of the chip sampler.

Very large flat chip: One with shape and dimensions based on those of the biggest chips in the largest size fraction of the chip samples.

In both tables the maximum flow rates are in bold. The gaps in the tables do not have any significance. Model runs were done to determine the relationship between the initial positions of the chip and the flow required to flush the chips into the annulus in the time between hammer blows. Once these relationships were determined for both bit and rockdrill combinations and the various sizes of chip there was no need for further runs. The flow rates do not increase and decrease smoothly with increasing initial position because of:

- The finite size of the flow rate increments in the model.
- Rounding-off errors.
- Changes in the cross sectional area available for flow. This explains the large change in flow rate for the 48 mm diameter bit between initial chip positions of 8 and 9 mm.

Table D3 Results from the model for the 48 mm diameter bit.

Initial position (mm)	Minimum flow rate (l/min.)		
	Minute cubic chip	Average large flat chip	Very large flat chip
0.25	7.793	12.998	-
0.375	10.471	-	-
0.5	10.447	12.678	-
0.75	10.491	12.372	-
1.0	10.428	12.155	-
1.25	-	11.77	-
1.5	10.373	11.803	-
1.75	-	11.822	-
2.0	10.285	12.141	-
2.25	-	12.127	-
2.5	10.249	12.102	-
2.75	-	12.353	-
3.0	10.173	12.298	-
3.25	-	12.231	-
3.5	10.136	12.154	-
3.75	-	12.324	-
4.0	10.055	12.22	-
4.25	-	12.107	-
4.5	-	12.154	-
5.0	9.839	11.934	-
6.0	-	11.699	-
7.0	9.39	11.461	-



CONTINUATION OF TABLE D3			
Initial position (mm)	Minimum flow rate (l/min.)		
	Minute cubic chip	Average large flat chip	Very large flat chip
8.0	9.166	11.253	-
8.5	-	11.669	11.827
8.75	-	12.118	12.724
9.0	8.8274	13.375	13.520
9.25	-	14.449	15.057
9.5	-	14.693	14.827
9.75	-	14.576	14.576
10.0	8.275	14.427	14.672
10.25	-	14.483	14.717
10.5	-	14.267	14.378
10.75	-	14.236	14.343
11.0	7.574	13.959	14.26299
11.5	-	13.701	13.975
12.0	6.793	13.29	-

In all the subsequent graphs the initial position of the chips was the position at which maximum flow was needed to flush the chip into the annulus in the time between hammer blows. Thus the initial positions were:

Very large flat chips, initial position = 9.25 mm;  
 Average large flat chips, initial position = 9.0 mm  
 Minute cubic chips, initial position = 0.75 mm.

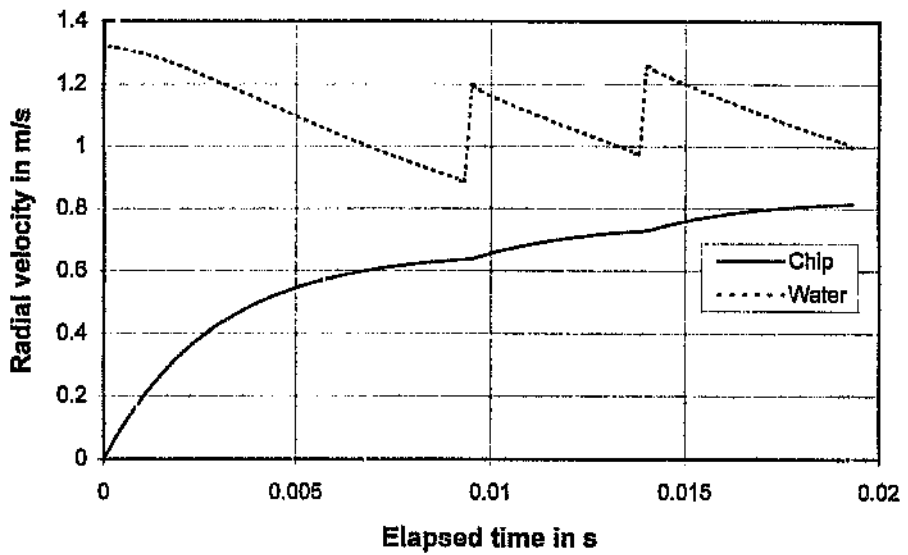


Figure D2 Velocity of flushing water and very large flat chip

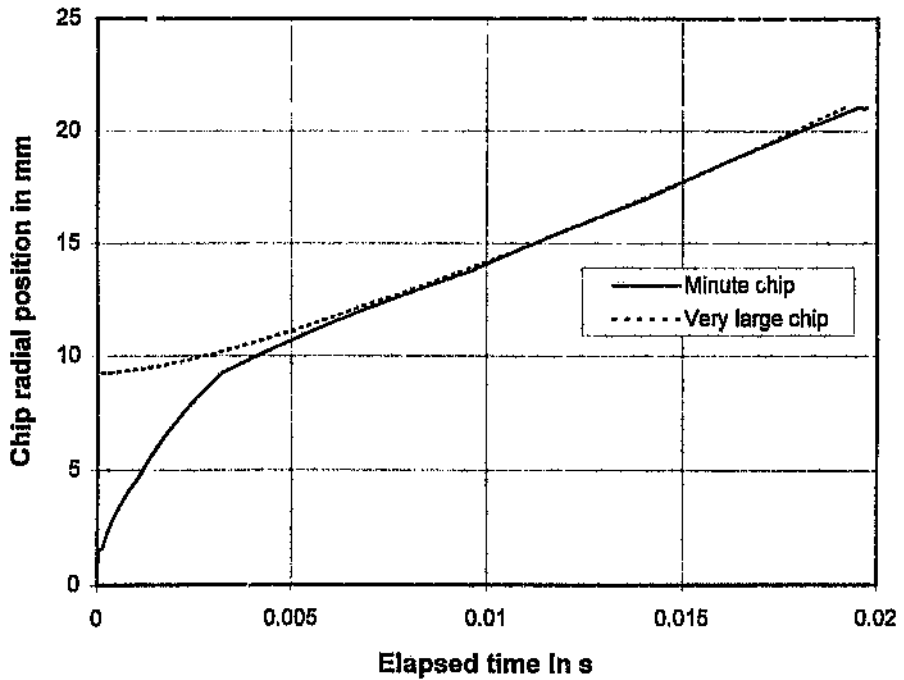


Figure D3 Chip displacement

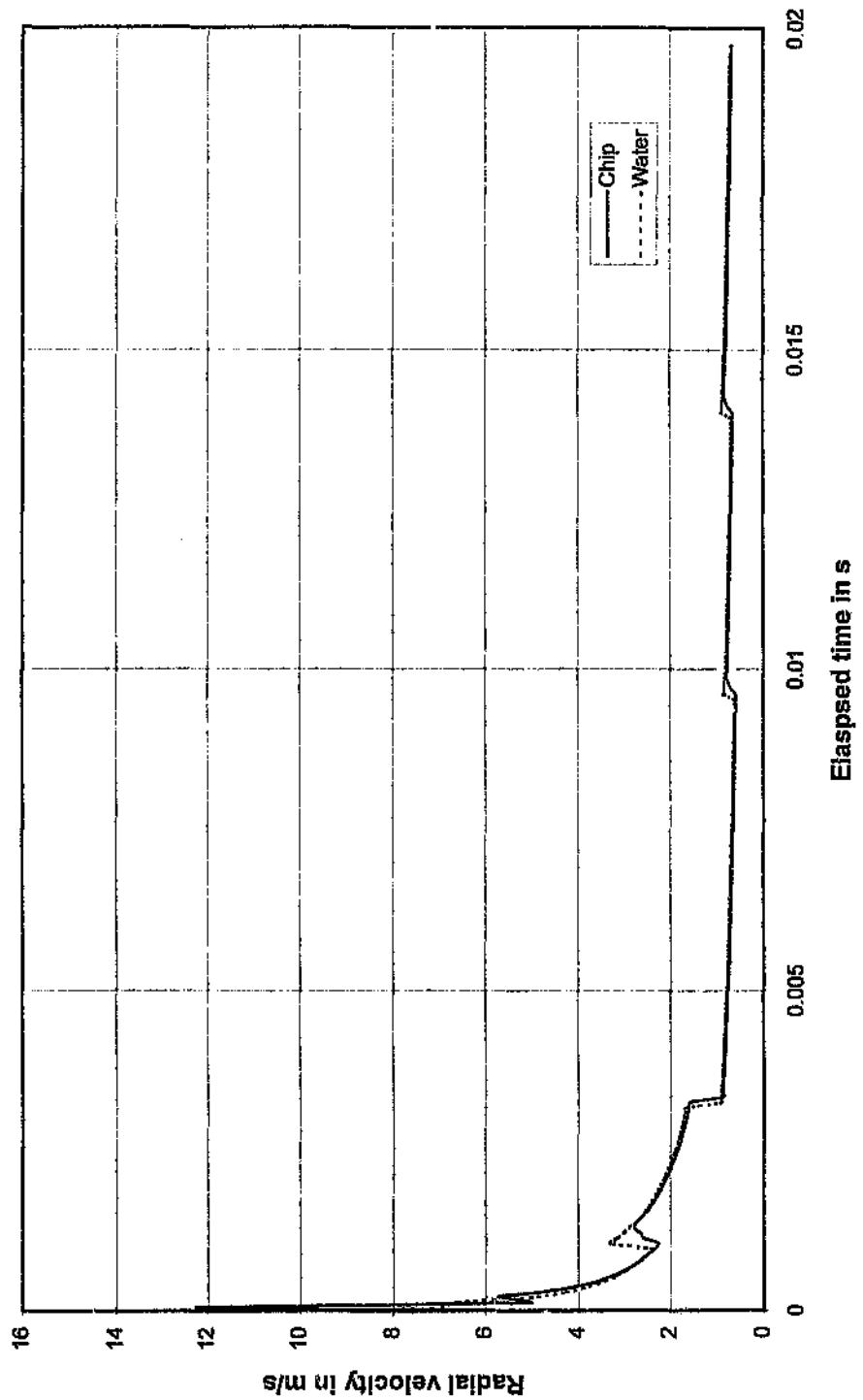


Figure D4 Velocity of flushing water and minute cubic chip

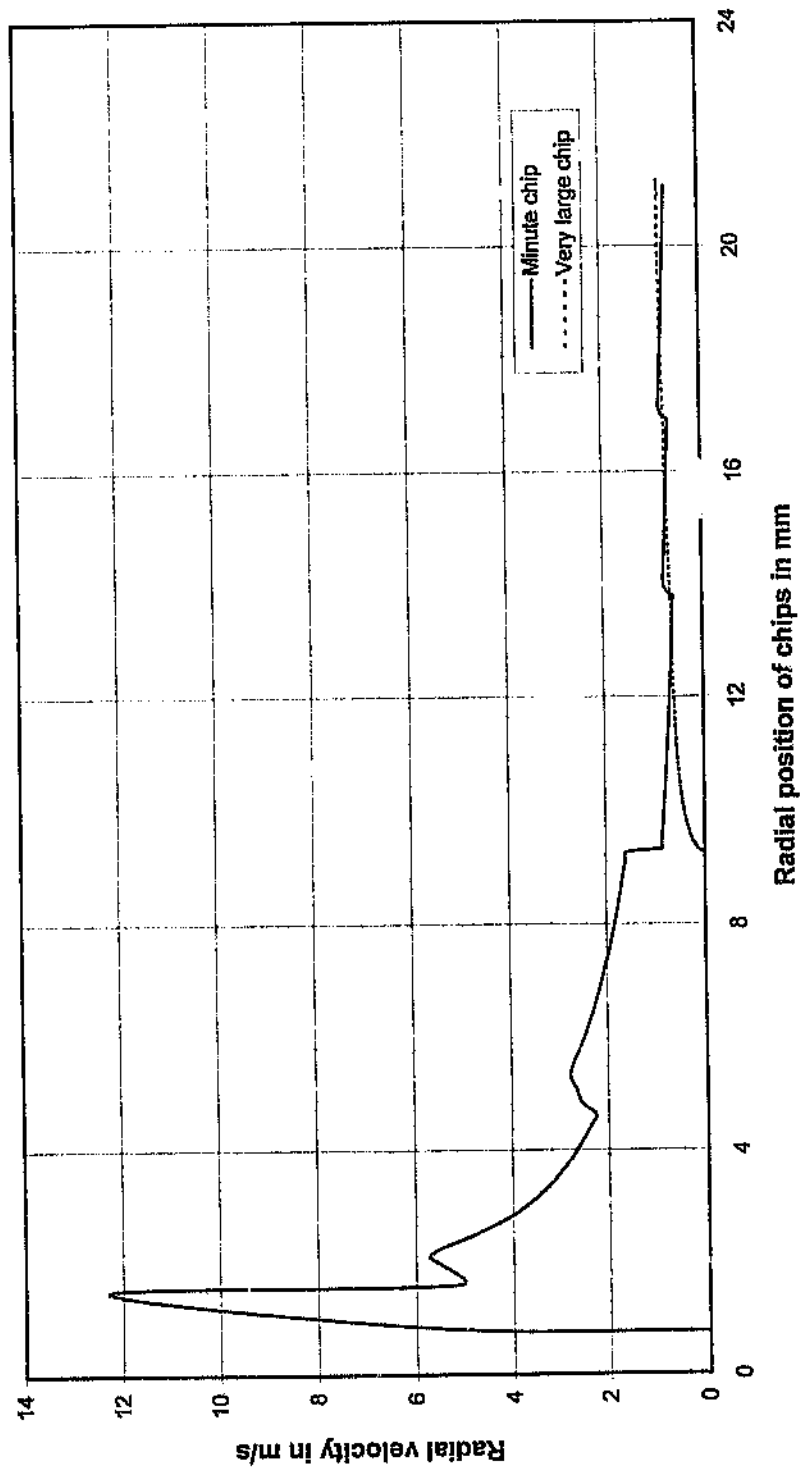


Figure D5 Effect of chip size on velocity

As before, the bold figures in the table below are maximum flow rates.

Table D4 Results from the model for the 36 mm diameter bit

Initial position (mm.)	Minute cubic chip	Average large flat chip	Very large flat chip
0.375	2.763	-	-
0.5	2.746	2.913	-
0.75	2.742	-	-
1.0	2.749	3.028	3.028
1.25	2.734	-	3.038
1.5	2.729	3.101	3.101
1.75	-	-	3.151
2.0	2.686	3.19	3.19
2.25	-	-	3.217
2.5	-	3.234	3.234
2.75	-	-	3.234
3.0	-	3.189	3.189
3.5	-	3.243	3.243
3.75	-	-	3.25
4.0	-	3.284	3.284
4.25	-	-	3.303
4.5	-	3.307	3.307
4.75	-	-	3.297
5.0	-	3.274	3.274
5.25	-	-	3.267
5.5	-	3.191	3.191

## D3 CHIP SIZES

The meanings of the headings in table D5 are:

Flow rate - Flushing flow.

Large fraction - Proportion of chips failing to pass through a 2 mm mesh.

Sum of 2 smallest fractions - Proportion of chips able to pass through a 0.25 mm mesh.

Smallest fraction - Proportion of chips able to pass through a 0.075 mm mesh.

In all cases the proportions were by mass.

Table D5 Chips produced by the 36 mm diameter bits

Flow rate (l/min)	Large fraction (%)	Sum of 2 smallest fractions (%)	Smallest fraction (%)
0.72	0.95	42.1	18.3
1.0	0.61	44.4	17.2
1.7	3.1	32.5	11.3
2.4	8.5	24.5	2.9
2.8	2.4	36.6	15.4
3.5	1.5	39.6	13.4
3.8	4.3	32.1	12.4
5.0	4.9	35.7	12.0
8.8	1.04	48.8	13.7
10.0	7.3	23.1	6.8
15.9	11.2	27.8	7.3
20.0	7.9	27.4	8.7

The headings in table D6 which are different from those in table D5 have the meanings listed overleaf.

No. - Number of samples obtained.

Mean of largest - Average of proportions of chips failing to pass through a 2 mm mesh.

Mean of sum of two smallest - Average of proportions of chips able to pass through a 0.25 mm mesh.

Mean of smallest - Average of proportions of chips able to pass through a 0.075 mm mesh.

Table D6 Chips produced by the 48 mm diameter bits

Flow rate (l/min)	No.	Mean of largest (%)	Mean of sum of two smallest (%)	Mean of smallest (%)
3.4	3	5.7	29.2	17.5
4.0	4	4.1	50.7	23.8
8.5	3	5.0	61.0	35.4
10.9	3	3.4	54.3	29.7
11.5	1	3.8	36.3	13.4
12.0	3	19.2	35.3	12.5
12.5	4	10.1	43.6	21.6
13.1	3	13.9	43.4	17.5
13.5	3	12.7	40.2	13.3
16.0	2	8.0	33.7	9.4
18.6	3	6.3	39.2	9.7
20.0	3	16.1	34.0	15.0
22.0	1	16.8	18.3	2.3
24.0	3	14.4	34.9	11.6
26.0	2	15.5	36.2	16.0
28.0	1	14.5	37.6	10.1
36.3	2	22.5	29.5	12.2

In most cases there was more than one set of data for each flow rate. Hence the data was averaged. For three flow rates only one set of data was available, therefore no averaging was possible. All proportions were by mass.



## REFERENCES

1. Davis, R.F., The conveyance of solid particles by fluid suspension, *Engineering*, 140, 1935, pg. 2. [Cited in Fish, B.J., Studies with water and air as flushing media in rock drilling, *Mine and Quarry Engineering*, July 1957, pp. 306-10].
2. Jain, C.K., Selection of air supply equipment for drilling of water wells, *Indian Mining and Engineering Journal*, Aug/Sept. 1985
3. Berson, R., *The Effect of Flushing Flow Rate on the Penetration Rate of 45 mm Button Bits*, Krugersdorp: Boart Longyear Research Centre Technical Note 85/13(E), 1985, pg. 6.
4. Berson, R., *Flushing Tests Carried Out on Button Bit Test Rig*, Krugersdorp: Boart Longyear Research Centre Report 84/2(E), 1984, pp 4-5.
5. McFadzean, S., *Calculation of Velocity of Slurry Past a Small Diameter Button Bit at Various Flow Rates*, Krugersdorp: Boart Longyear Research Centre Report 80/13(E), 1980, Appendix D.
6. Berson, R., *Flushing Tests Conducted on 45mm Bits in a Simulated Laboratory Apparatus*, Krugersdorp: Boart Longyear Technical Note 84/6(E), 1984, pg. 6.
7. Williams, D.S., *Flushing Tests Using Model Button Bits in a Flushing Jig*, Krugersdorp: Boart Longyear Research Centre Report 82/5(E), 1982, pg. 2.
8. Schwartz, I.F., Private Conversation, April 1997.
9. Brewitt, P., Private Correspondence, July 1997.

10. Loots, D.J., *Private Correspondence*, June 1997.
11. Wiles, R.J., *Pneumatic Conveying of Solids (Course Notes)*, St. Lucia (Australia): Department of Chemical Engineering, University of Queensland, 1982.
12. Marcus, R.D., Leung, L.S., Klinzing, G.E. and Rizk, K., *Pneumatic Conveying of Solids*, 1st ed. London: Chapman and Hall, 1990, pp 106.
13. Bain, A.G. and Bonnington, S.T., *The Hydraulic Transport of Solids by Pipeline*, 1st ed. Oxford: Pergamon, 1970, pg. 27.
14. Zandi, I. and Govatos, G., *Proceedings of ASCE (Hydraulic Division)*, May 1967 [Cited in Bain and Bonnington<sup>(13)</sup>].
15. Graf, W.H., *Hydraulics of Sediment Transport*, 1st ed. New York : McGraw Hill, 1971, pg. 50.
16. Douglas, J.F., Gasiorek, J.M. and Swaffield, J.A., *Fluid Mechanics*, 1st ed. London : Pitman, 1979, pg. 309.
17. Timoshenko, S.P., and Goodier, J.N., *Theory of Elasticity*, 3rd ed. Tokyo: McGraw Hill International, 1982, pp 492 - 504.
18. Enick, R. and Klinzing, G.E., *Proceedings of Fine Particle Society*, 1985 [Cited in Marcus et al.<sup>(4)</sup>]
19. Daugherty, R.L. and Franzini, J.B., *Fluid Mechanics with Engineering Applications*, 1st ed. Tokyo: McGraw-Hill Kogakusha, 1977, pg. 295.
20. Beddow, J.K., Fong, S.P. and Vetter, A.F., *Powder Technology*, vol. 22, no. 17, 1979 [Cited in Marcus et al.<sup>(4)</sup>]

21. Gieck, K, *Technical Formulae*, 5th English language ed. Heilbronn : Gieck-Verlag, 1982, pg. L5.

**Author: Kilfoil, Arthur Mark.**

**Name of thesis: Water flushing of rock chips from horizontal holes drilled by rotary percussion.**

***PUBLISHER:***

**University of the Witwatersrand, Johannesburg**

**©2015**

***LEGALNOTICES:***

**Copyright Notice:** All materials on the University of the Witwatersrand, Johannesburg Library website are protected by South African copyright law and may not be distributed, transmitted, displayed or otherwise published in any format, without the prior written permission of the copyright owner.

**Disclaimer and Terms of Use:** Provided that you maintain all copyright and other notices contained therein, you may download material (one machine readable copy and one print copy per page) for your personal and/or educational non-commercial use only.

The University of the Witwatersrand, Johannesburg, is not responsible for any errors or omissions and excludes any and all liability for any errors in or omissions from the information on the Library website.